
The Contribution of Antarctic Peninsula Ice to Sea Level Rise



E M Morris

British Antarctic Survey
Natural Environment Research Council

Cover Photograph: Collecting firn cores in the Antarctic Peninsula to monitor trends in snow accumulation rate.

**The Contribution of Antarctic Peninsula Ice
to Sea Level Rise**

**Report for the Commission of the
European Communities Project
EPOC-CT90-0015**

Edited by

E M Morris



Published by the British Antarctic Survey
Natural Environment Research Council
High Cross
Madingley Road
Cambridge, CB3 0ET, UK

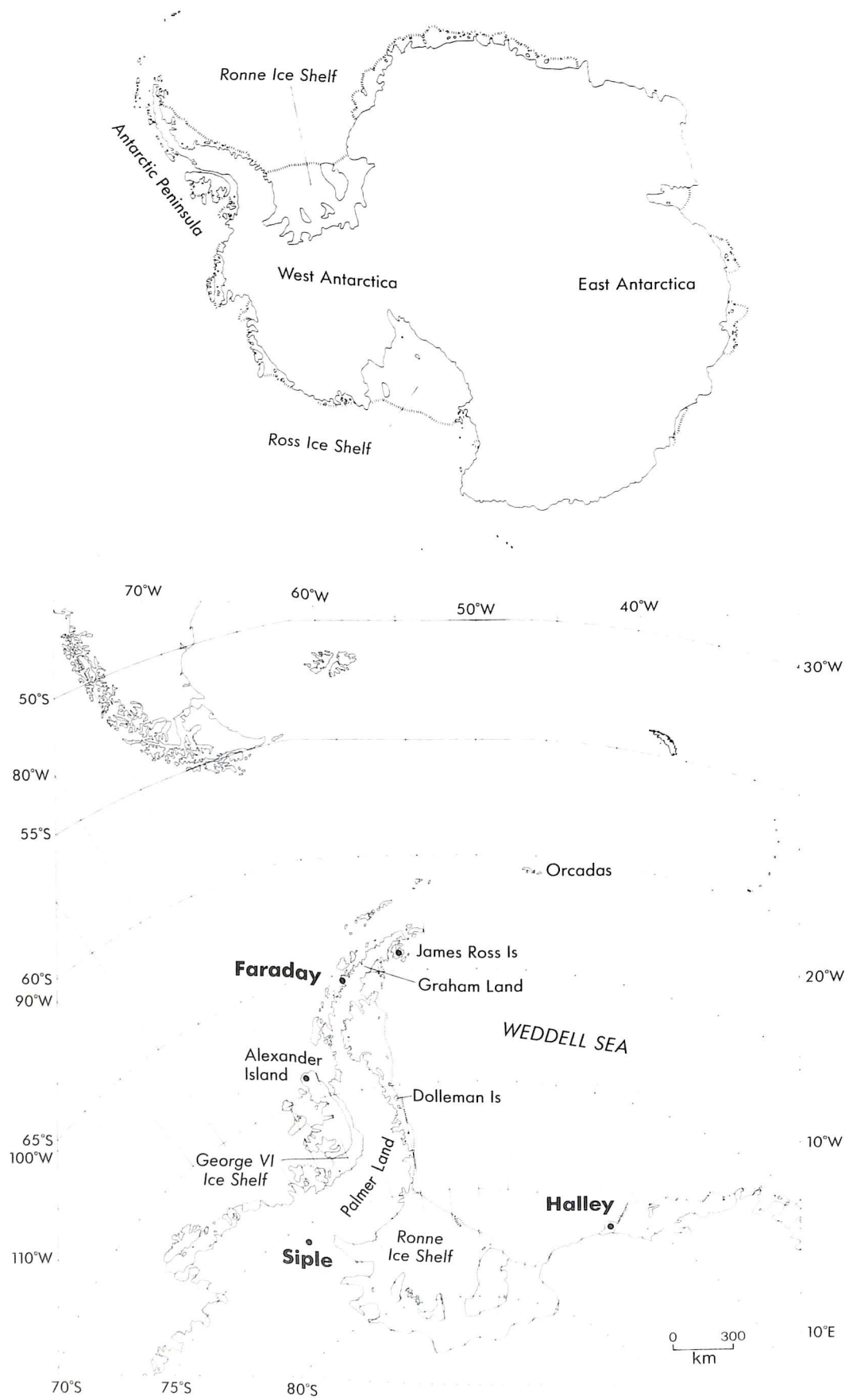
© British Antarctic Survey

First Published 1992

ISBN: 0-85665-149-4

Contents

Introduction (<i>E M Morris</i>)	1
Surface Mass Balance of the Antarctic Peninsula Ice Sheet (<i>R M Frolich</i>)	3
Spatial Temperature and Accumulation Rate Variations in the Antarctic Peninsula (<i>D A Peel</i>)	11
Snow Surface Temperatures in West Antarctica (<i>E M Morris and D G Vaughan</i>)	17
Global Climate Models and Antarctica (<i>W Connolley</i>)	25
Estimating Ice Sheet Response to Climate Change (<i>R C A Hindmarsh</i>)	27
Sea Level and the Ice Shelves of the Antarctic Peninsula (<i>D G Vaughan</i>)	35



The Antarctic Peninsula Region

The Antarctic Peninsula region showing the locations of selected features and stations mentioned in the text.

INTRODUCTION

E M Morris

This collection of papers forms an interim report on research undertaken at the British Antarctic Survey (BAS) in support of the project "Climate Change, Sea Level Rise and Associated Impacts in Europe" funded by the Commission of the European Communities (CEC). The aim of the BAS research is to predict the contribution to sea level rise from changes in the volume of ice in the Antarctic Peninsula over the next 100 years.

The contribution of the Antarctic as a whole to future sea level rise has been estimated by the Intergovernmental Panel on Climate Change (IPCC) as $-0.3 \pm 0.3 \text{ mm a}^{-1} \text{ } ^\circ\text{C}^{-1}$. For a warming of 2°C over 40 years, for example, this implies a reduction in sea level of $24 \pm 24 \text{ mm}$. Sea level falls because warmer temperatures over the Antarctic bring increased accumulation, at least until the temperature has risen to the point where summer melting can occur, as in Greenland. The IPCC estimate was based on the assumption, first suggested by Robin, that over the whole of Antarctica (i) the change in accumulation is proportional to change in saturation mixing ratio above the surface inversion layer and (ii) that there is a linear relation between mean annual surface air temperature and saturation mixing ratio. Furthermore, it was assumed that the ice sheet is now in equilibrium and that its dynamic response to future climate change can be ignored on the 100 year time scale under consideration.

Although these are reasonable hypotheses for the main area of the continent they do not necessarily apply to the Antarctic Peninsula with its complex mountainous terrain, relatively warm climate and smaller, more rapidly responding ice masses. For this reason a detailed study of the Antarctic Peninsula ice sheet is sorely needed to place the IPCC predictions on a firmer foundation.

The mountain chain which forms the Antarctic Peninsula stretches 1500 km northwards from Ellsworth Land with peaks rising to over 2500 m asl. It acts as a major barrier to tropospheric circulation over the Southern Ocean. On the east side of the Peninsula extensive and persistent sea ice in the Weddell Sea leads to temperatures which are 7°C lower than at the same latitude on the west side and ice shelves extend 350 km further north. Accumulation rates over the Antarctic Peninsula are high; although the area is only 7% of the area of Antarctica it receives some 23% of the total surface accumulation. About 2% of the Peninsula area has a mean annual temperature greater than -11°C and periods of melting during the summer.

In the first paper of this report **Frolich** uses existing data on accumulation in the Antarctic Peninsula to produce a new estimate of the surface mass balance of Antarctica. His figure of $2144 \pm 240 \text{ Gt a}^{-1}$ is 468 Gt a^{-1} less than the estimated output of ice from the continent. This difference is not significant, since the error in the output is of same order. Thus at the moment the assumption that the ice sheet as a whole is in equilibrium with the present climate cannot be disproved.

Peel has looked at high quality data from sites in the Antarctic Peninsula where both accumulation and mean annual temperature have been determined. He has established that the Robin relation is applicable for areas with mean annual temperatures of less than -11°C . This is encouraging as it means that for most of the area of the Antarctic Peninsula the increase of accumulation associated with a warmer climate can be estimated using the methods already established by the IPCC. Peel also examines the temporal trend in accumulation rates and shows that at several sites they have increased by around 20% since about 1950.

The distribution of mean annual temperature over the Antarctic Peninsula can be determined from meteorological records and from measurements of snow temperature made in boreholes below the penetration depth of the annual temperature wave. **Morris and Vaughan** have analysed borehole data

taken on traverses of the Antarctic Peninsula and Filchner-Ronne Ice Shelf area to determine lapse rates with latitude, longitude, altitude and time.

Given this improved understanding of climatic processes in the Antarctic Peninsula region the next stage is to try to determine the detailed climatic response to the various standard scenarios for greenhouse gas emissions. At the start of the project we had hoped that the predictions of General Circulation Models (GCMs) could be used to give an indication of climate change for these scenarios on the 500 km grid scale used in the models. The sub-grid scale variations would then be established using the empirical relations derived for the present day climate. However, as **Connolley** explains, there are flaws in current models which suggest that they can only be used as a guide to future regional rather than grid-scale climate change. It will be necessary, therefore, to establish relations between local climate data and regional parameters. This work is in progress.

In the IPCC calculations it was assumed that the dynamic response of the ice to increasing surface temperature and accumulation rate could be ignored. **Hindmarsh** has developed a mathematical model of the Antarctic Peninsula Ice Sheet which indicates that the time scale for this ice mass to reach equilibrium under changed climatic conditions is of the order of 500 to 1000 years. However, this does not mean that its dynamics need not be considered on the 100 year time scale with which this project is concerned. Hindmarsh shows that the initial response of the ice sheet to increased accumulation is an increased downward vertical velocity; the ice sheet profile adapts to the new conditions on a time scale of 65 to 250 years. This analysis is being extended to include an improved treatment of the effects of increasing temperature on the flow law of ice.

In the last paper, **Vaughan** discusses the role of ice shelves. Although changes in volume of floating ice have no direct effect on sea level, there are indirect processes which could allow changes in ice shelf extent or thickness to alter the volume of grounded ice and thus contribute to sea level change. Indeed, it has been suggested that the removal of the restraining back pressure of the Filchner-Ronne and Ross ice shelves on the large ice streams of West Antarctica could initiate a rapid collapse of the West Antarctic Ice Sheet and sea level rise of around 5 m. Vaughan shows that although the ice shelves of the Antarctic Peninsula are retreating in response to the warming climate of the last 40 years, there has been no noticeable contribution to sea level rise and none should be expected in the future.

Editor's Acknowledgements

This report was prepared for printing by Anne Hall, aided by Sue Robertson and Tony Sylvester. Both editor and authors acknowledge with gratitude the skill and enthusiasm shown by Anne and her team. The project (EPOC-CT90-0015) is supported by the Commission of the European Communities, whose funding made the production of this volume possible.

THE SURFACE MASS BALANCE OF THE ANTARCTIC PENINSULA ICE SHEET

R M Frolich
British Antarctic Survey
Natural Environment Research Council
High Cross, Madingley Road
Cambridge, CB3 0ET
United Kingdom

Abstract

Total surface mass balance on the Antarctic Peninsula Ice Sheet is estimated to be $294 \pm 36 \text{ Gt a}^{-1}$ for conterminous grounded ice and $491 \pm 79 \text{ Gt a}^{-1}$ for all ice surfaces combined. Equivalent figures for the whole Antarctic of $1572 \pm 165 \text{ Gt a}^{-1}$ and $2144 \pm 240 \text{ Gt a}^{-1}$ are obtained by updating a previous estimate. Major contributors to uncertainty are the sparse dataset, which contains strong temporal and spatial biases, and the poor parameterisation of ablation. Since the ice sheet contributes some 20% to the Antarctic surface mass balance (greater than current estimates of the total Antarctic imbalance) and lies in a region thought to be particularly sensitive to climate change, improvements to the dataset and our understanding of climate sensitivity are urgently needed.

1. Introduction

The Antarctic Peninsula Ice Sheet (depending on how it is defined) includes up to 7% of Antarctica's area and receives up to 23% of its surface accumulation. Since the region's proximity to the sea and low latitude also make it the most likely part of Antarctica to show signs of rapid climate change (e.g. Mercer, 1978), there is a need to establish a benchmark for climatic parameters here as soon as possible. Indeed, decay of ice shelves at their climatic limit (Doake and Vaughan, 1991), increasing surface temperature (Jones and Limbert, 1987; Morrison, 1990) and increasing surface accumulation (Peel, this report) have all been observed in the last few decades.

The Antarctic Peninsula (Figure 1) is sometimes neglected in calculations of the overall mass balance of the Antarctic Ice Sheet. Giovinetto and Bentley (1985), for example, presented a compilation for Antarctica that excludes over 20% of the Antarctic Peninsula region (the catchments associated with the coastline between points I and J in Figure 2). They pointed out the rugged terrain and said that little was to be gained from applying the few measurements made on Antarctic Peninsula escarpment to the whole escarpment. But high plateau and ice shelf make up the majority of the surface and are sufficiently well covered by measurements for rough estimates of their contributions to be made. Even on escarpment, Peel (this report) shows that net accumulation in a particular regime may vary regularly with position or elevation, so the calculation of a regional total is far from worthless. Assessing the net effect on the ice sheet of any

climatic change clearly requires well designed fieldwork and sophisticated mathematical modelling. In the meantime, however, this paper describes a simple attempt to estimate the current total surface mass balance of the ice sheet and, equally importantly, to identify the major sources of uncertainty in the total and their magnitudes.

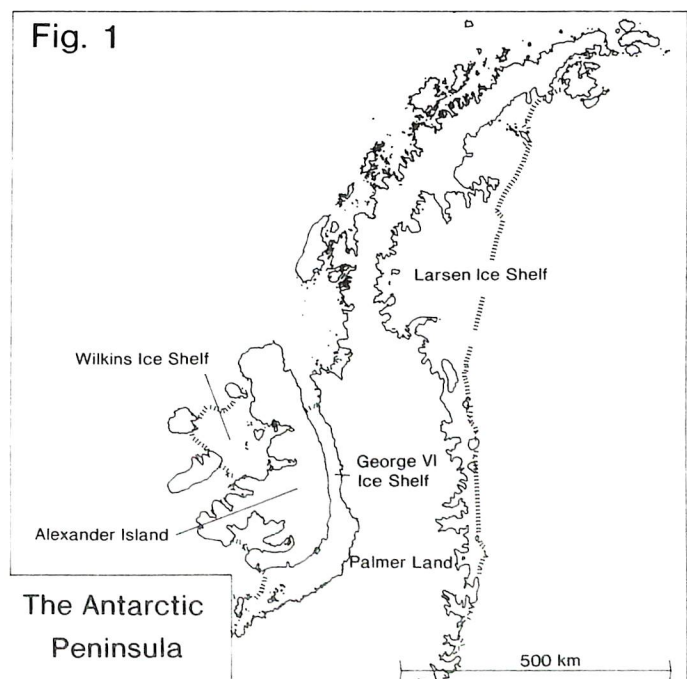


Figure 1. Location of places referred to in text

2. Definitions

The Antarctic Peninsula Ice Sheet can be defined in a hierarchy of different ways. Following Giovinetto and Bentley (1985), I use the term *conterminous grounded ice* to describe that part of the ice surface connected to the rest of Antarctica by grounded ice (rather than by only ice shelf or open water). The term *grounded ice* includes the *conterminous grounded ice*, plus the ice islands and ice rises, and *all ice surfaces* includes the *grounded ice* plus the floating ice shelves.

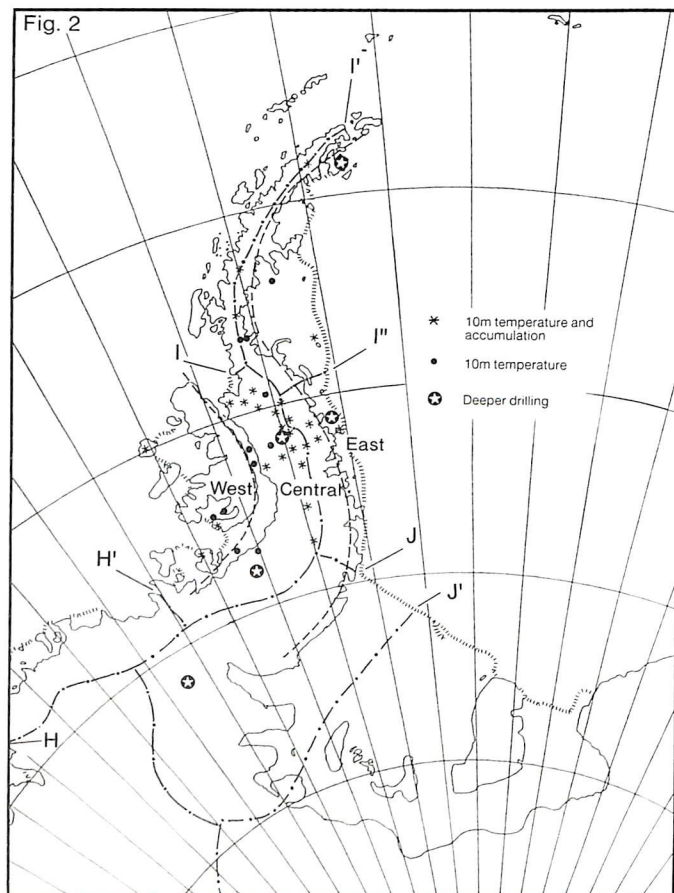


Figure 2. Distribution of sampling sites for surface mass balance (after Peel, this report). Catchment basins (after Giovinetto and Bentley, 1985) are delineated by alternate dots and long dashes, and climatic regimes by short dashes.

Following Paterson (1981), *surface mass balance* (or *net accumulation*) at a point is defined as the net addition of material over the year to a unit area of the ice sheet surface. It is the difference between total accumulation (e.g. snowfall, drift and condensation) and total ablation (e.g. meltwater run-off, evaporation and wind scouring). Point measurements of surface mass balance (which may be negative) can then be interpolated and integrated over an ice sheet to give the surface mass balance for the whole ice sheet. The

total mass balance of the ice sheet is then the difference between the integrated surface mass balance and the total attrition due to ice flow across grounding lines (or iceberg calving if the ice sheet is defined to include ice shelves) and basal melting.

It is also necessary to distinguish those ice surfaces where any summer meltwater is contained entirely within the previous winter's snow from the 20 000 km² (2% of the total area) where meltwater either percolates more deeply into the snowpack or runs off completely. This is because of difficulties in interpreting stratigraphy from sites strongly influenced by surface melting and the possibility of significant ablation in this regime (where such melting occurs it also tends to be very variable, in both time and space). The boundary between the two regimes on the Antarctic Peninsula coincides roughly with the -11°C in situ mean annual isotherm (Reynolds, 1981). Where the mean annual surface temperature is below -11°C, surface mass balance will be very close to the total accumulation.

To avoid a somewhat arbitrary boundary with the rest of the Antarctic continent, the region has been taken to include all of the catchments associated with the coastline between H and J' in Figure 2. I present new figures for surface area and total mass balance only for catchments H'-J, however.

I have ignored the fact that the boundaries of the various ice sheet components are subject to change over time, through changing sea level, the advance or retreat of ice fronts and grounding lines, or the breaking up of whole ice shelves, and that the small percentage of the region that is ice free in summer can also change, particularly close to the coast.

Place names used are those which appear on the 1:3 000 000 British Antarctic Territory map, 1981 (British Antarctic Survey, Misc. 2 edition 1). Where available, the associated 1:500 000 topographic base maps were used to measure areas in 500 metre altitude intervals, otherwise the 1:3 000 000 map was used. Because these maps represent a synthesis of information gathered over a number of years, calculated surface areas, particularly in the case of ice shelves, will not generally be contemporaneous with balance measurements.

Some, if not most, of the winter precipitation on areas that are ice free in summer will melt and refreeze in the snowpack rather than running off into the sea or evaporating. Since measurements are generally made at sites away from rock outcrops and therefore not influenced by this process, it will be necessary to assign a non-zero accumulation rate to the areas that are ice free in summer.

3. Data sources

There is an average of one measurement of surface mass balance for every 10 000 km² of the Antarctic Peninsula Ice Sheet surface. Although this density is similar to that over the Antarctic continent as a whole, climatic parameters which tend to vary slowly and smoothly in the continental interior can vary far more rapidly in the Antarctic Peninsula because of the rugged terrain and juxtaposition of maritime and continental climates there. Total accumulation ranges from less than 200 kg m⁻² per year at some sites on the plateau of Palmer Land to over 1000 kg m⁻² per year at some sites on the west coast. In some areas strong ablation means that negative balances occur, for example, close to the snouts of the few glaciers that terminate before reaching the coast in the north-west, but the total area involved is likely to be small.

Peel and Clausen (1982) and Peel (this report) discuss in detail the sources of most of the balance data used here and their individual reliabilities. Peel uses measurements from ice cores (a total of about 30 observations) to examine the variation of mass balance in the Antarctic Peninsula region (Figures 2 and 3). Other measurements, available from pit stratigraphy and shallow seismic refraction (a further 30 or so observations) and stakes, are avoided because of difficulties in their interpretation. Since Peel also rejects observations from sites warmer than -11°C because their stratigraphies may be influenced by meltwater, these results cannot be expected to adequately describe mass balance where ablation is dominant.

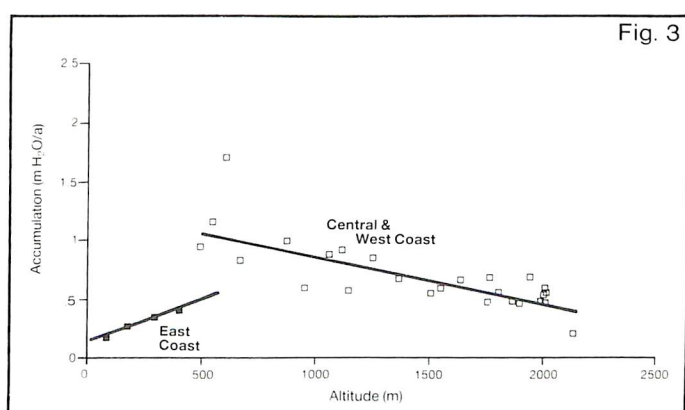


Fig. 3

Figure 3. Mean annual snow accumulation rate in the Antarctic Peninsula as a function of altitude (after Peel, this report).

Some parts of the region are very poorly sampled. The distribution of sites is dominated by coastal and plateau sites, with few on steep escarpment or in south eastern Palmer Land. Poor coverage forced Peel to

include the measurements of high net accumulation on the islands to the west of Alexander Island, but without any real indication of how mass balance varies between there and the Antarctic Peninsula itself. Some measurements from Wilkins Ice Shelf (Vaughan et al., in press) suggest that mass balance may fall to perhaps 500 kg m⁻² a⁻¹ away from the coast where the cores used by Peel were taken.

Potter et al. (1984) used some of the shallow seismic refraction experiments, pit stratigraphy and stake data excluded by Peel to supplement core data from Palmer Land and George VI Ice Shelf in their calculation of the total mass balance for the catchment area of the ice shelf.

The relatively long history of fieldwork around the Antarctic Peninsula and the fact that deep ice cores can provide records going back centuries raise the question of how to combine such data. Two possibilities are: reducing observations to a common epoch by removing a secular variation of accumulation (either directly or through a proxy such as temperature); or weighting values that are long term averages from deep ice cores more heavily than those from other sources. I have attempted neither here, so the final values are inevitably temporally, as well as spatially, biased and not strictly suitable for a single figure representing a present day benchmark against which to measure future changes. What is possible, however, is to give a rough figure for the total mass balance and identify the major sources of uncertainty.

4. Spatial variation of mass balance.

Peel (this report) gives the following linear regressions against altitude of mass balance measurements made on deep and shallow cores. The data from the east-coast sites, which show an increase of accumulation with altitude (at least up to 400 metres), are separated from those in the West and Central zones (Figure 2), which show the expected decrease associated with a decreasing temperature and air moisture content (Figure 3). Peel tentatively attributes the anomalous east-coast behaviour to a high frequency of stable temperature inversions over the Weddell Sea zone.

Zone	Present mass balance (mean) m water/a	Regression against altitude m water/a/km
West	1.26 ± 0.39	1.32 - 0.45.Alt
Central	0.61 ± 0.16	1.32 - 0.45.Alt
East	0.31 ± 0.08	0.15 + 0.64.Alt

Note: 1 m water/a is equivalent to 1000 kg m⁻² a⁻¹.

With the data divided between the two distinct climatic regimes, mass balance correlates well with altitude ($r=0.79$ for the combined West and Central areas and $r=0.97$ for the East). Such strong correlations suggest that little would be gained from including more variables, such as latitude or longitude (in this case correlated with altitude), or higher order terms, at least until more data become available from poorly sampled areas. A continuous function can be formed by making the two relations intersect at an elevation of about 1075 metres on the eastern side of the peninsular crest (Figure 3). For simplicity, the boundary between the two regimes has been assumed to be at 1000 metres. This small error, which is incurred over a small area, will be insignificant compared with that due to the complete lack of data at this altitude on the east coast.

5. Summation

The integration of point mass balance measurements was performed manually, measuring areas from maps, correcting for scale distortions and weighting with the balance estimate for the appropriate climatic regime and 500 metre wide altitude interval. Most ice sheet

surfaces (as distinct from ice streams or ice shelves) are convex upward, so the integration in any elevation interval should be biased towards the higher elevations. This will tend to make my estimates of total balance too high everywhere except within the first 1000 m above sea level on the east coast. Any such error is unlikely to be a major source of uncertainty, however. I have assumed that all ice shelf surfaces are at sea level. I have also assumed that the dependence of mass balance on altitude for ice-free areas and for areas where the mean annual temperature is above -11°C is given in both cases by Peel's regressions, but with proportional reductions to account for ablation.

The area of bare rock is difficult to assess accurately, but is approximately 30 000 km², mostly below 1000 metres elevation. I have assumed that only 80% of the snowfall here finds its way into the nearby snowpack through either melting or drifting.

The area subject to meltwater runoff is probably only a small fraction of that where the mean annual temperature is above -11°C .

Catchment	Conterminous grounded ice	Ice Islands	Ice Shelves	Totals
*H-H'	65.4 ± 6.5 (82)	-	51.0 ± 5.1 (51)	116.4 ± 11.6 (133)
*H'-I	49.8 ± 5.0 (113)	-	48.4 ± 4.8 (121)	98.2 ± 9.8 (234)
#H'-I (GIS&C)	41.8 ± 2.5 (77.2)	0 (0)	11.1 ± 1.5 (24.9)	52.8 ± 2.8 (102.8)
H'-I (ex. GIS&C)	40.0 ± 7.4 (48.5)	56.5 ± 20.0 (60.4)	33.3 ± 12.5 (31.5)	132.4 ± 35.9 (140.4)
H'-I (GIS&C)	57.2 ± 10.0 (77.9)	0 (0)	32.2 ± 12.0 (24.4)	89.4 ± 19.8 (102.3)
I-I'	22.8 ± 5.2 (31.0)	8.6 ± 2.9 (9.5)	0 (0)	31.4 ± 7.3 (40.5)
I'-I''	18.7 ± 3.4 (40.5)	1.0 ± 0.3 (3.4)	11.5 ± 3.0 (77.6)	31.2 ± 6.0 (121.5)
I''-J	31.5 ± 7.0 (58.5)	0.3 ± 0.1 (1.1)	2.7 ± 0.7 (18.2)	34.5 ± 7.0 (77.8)
*J-J'	74.1 ± 7.4 (249)	-	21.1 ± 2.1 (124)	95.2 ± 9.5 (373)
Totals				
H'-J	154 ± 23 (256)	66 ± 21 (74)	59 ± 16 (152)	279 ± 60 (482)
H-J'	294 ± 36 (587)		197 ± 43 (401)	491 ± 79 (988)

Areas in 1000 km² are in brackets.

Figures (converted to Gt a⁻¹) from Potter et al. (1984). GIS&C refers to George VI Ice Shelf and catchment.

* From Giovinetto and Bentley (1985). Figures are for conterminous grounded ice and for ice islands, ice rises and ice shelves combined.

Table 1. Estimates of total surface mass balance in Gt a⁻¹ in catchments H-J'.

Where melt percolates deeply into the snowpack it still contributes to accumulation, so the presence of summer melting does not mean that net accumulation is negative; in most cases it will not be. To allow for significant ablation, I have reduced the estimates of average mass balance in these areas to 80% of those on colder surfaces in the same regime.

Mass balance totals for the different ice surfaces are shown in Table 1. Also shown are the figures from Potter et al. (1984) for the catchment area of George VI Ice Shelf and the corresponding figures obtained using Peel's regressions. The substantial difference is due mainly to the precipitation shadow that exists to the east of Alexander Island and to the loss of surface melting through evaporation and run-off via moulins in the ice shelf. The figures of Potter et al. (1984) are the more reliable, being derived by fitting a smooth function of latitude, longitude, elevation and their second order combinations to 26 local observations. To provide the best overall estimate I have therefore used their figures where appropriate and Peel's regressions elsewhere.

6. Errors

Using the standard deviations of accumulation measurements from the different regimes, Peel suggests that the uncertainty in accumulation estimates varies as follows: West, 31%; Central, 17%; East, 26%. Although it may be argued that better measures would be the standard deviations from the regression lines, both measures ignore the poor coverage and strong spatial and temporal biases in the data. It is these which probably contribute more to the uncertainty in the final totals. If ice shelves are included, Wilkins Ice Shelf must be the biggest source of uncertainty, followed by Larsen Ice Shelf. In both cases, changes of area, poor coverage and uncertainty about the amount of melting and runoff into the sea through moulins are important. For grounded ice, the biggest contributor to uncertainty is Alexander Island, and for the conterminous grounded ice alone, south eastern Palmer Land and those areas subject to significant ablation in the north and possibly the extreme west.

I have not attempted an explicit treatment of ablation or run-off, but merely estimated mass balance in areas subject to some surface melting by modifying a relation between accumulation and altitude derived from regions with no melting. Because this is so crude, I have allowed a margin of error of 20% either side of the 80% chosen as the appropriate proportion of the estimates from Peel's regressions. I have allowed a similar 20% error margin in the case of the contribution from ice free areas.

For the area determinations I have allowed 2% for grounded ice and 4% for ice shelves.

In combining the various error terms I have allowed for some independence; for example, between area estimates and average accumulation rate, but not between accumulation rates for different altitude intervals in the same regime. It is worth noting that the resulting range still just excludes the possibility that average mass balances on Wilkins Ice Shelf and the low lying parts of Alexander Island are as low as the figures quoted by Vaughan et al. (in press) or those used by Giovinetto and Bentley (1985).

7. Comparison with previous estimates and implications for Antarctic mass balance

Doake (1984) included a figure of $226 \text{ km}^3 \text{ a}^{-1}$ (or Gt a^{-1}) of water equivalent for the total annual accumulation on the Antarctic Peninsula Ice Sheet (taken in this case to mean all grounded ice north of an arbitrary line between Eltanin bay on the Bryan Coast, through 75°S , 80°W , to the most northerly point on the grounding line of Evans Ice Stream). Doake's figure was produced by dividing some 60 observations among ten distinct regions: four either side of the Antarctic Peninsula crest as far south as 75°S , one south of 75° and one containing the islands to the west of Palmer Land. Where there was a significant trend in accumulation with altitude, the total area in each region was divided into 500 m altitude intervals and weighted with the appropriate accumulation estimate from a linear regression. Otherwise the average of all observations from that region was applied to the whole region. Ablation was not explicitly considered and no error estimate was given.

If Peel's regressions can describe surface mass balance in the part of catchment J-J' included by Doake, then the figure for all grounded ice to compare with Doake's of 226 Gt a^{-1} is 268 Gt a^{-1} . Alternatively, removing from Doake's figure the contribution from catchment J-J' of roughly 30 Gt a^{-1} gives a total of 196 Gt a^{-1} for catchments H'-J (cf. 223 Gt a^{-1} here). Even though the discrepancies are about 15%, they are probably not significant, being mainly attributable to the large poorly constrained contribution from catchment H'-I. The totals for the other catchments agree far more closely.

I estimate that catchment H'-I contributes 183 Gt a^{-1} , or about 35%, to the Antarctic Peninsula total for all ice surfaces. This figure is nearly twice that quoted by Giovinetto and Bentley (1985). The difference appears to be due to them adopting an average net accumulation in this catchment of about $400 \text{ kg m}^{-2} \text{ a}^{-1}$.

I can only assume that they have rejected the measurements of accumulation rates of over 1 m a^{-1} on the islands to the west of Alexander Island, believing they are unrepresentative. Their average of $800\text{-}1000 \text{ kg m}^{-2} \text{ a}^{-1}$ for the adjacent catchment, H-H', seems inconsistent with this explanation, however, so I believe their total for catchment H-I may be underestimated by as much as 50%. Catchments I'-J, ignored by Giovinetto and Bentley (1985), contribute a further 97 Gt a^{-1} , or roughly 4% of the Antarctic total for all ice surfaces. If these discrepancies are viewed as corrections to the totals of Giovinetto and Bentley for the whole Antarctic, then new estimates over the various ice surfaces are:

Conterminous grounded ice	
1572 ± 165	(1468 ± 150) Gt a^{-1}
All ice surfaces	
2144 ± 240	(1963 ± 190) Gt a^{-1}

(Figures in brackets from Giovinetto and Bentley, 1985.)

8. Conclusions

Despite non-simultaneous measurements with poor coverage and strong spatial biases, it is possible to derive a useful figure for the total surface mass balance over the variously defined Antarctic Peninsula Ice Sheets. For the largest defined ice sheet, the total balance is $458 \pm 79 \text{ Gt a}^{-1}$, or 23% of the Antarctic total. When this figure is used to update that of Giovinetto and Bentley (1985) of 1963 Gt a^{-1} for the whole Antarctic Ice Sheet, the final total of 2144 Gt a^{-1} is probably the most reliable estimate available.

A number of weaknesses can be identified. For example, more sophisticated alternatives to the treatment presented here are possible, differing in the way in which mass balance measurements are interpolated, and in the way in which areas are calculated. The two extremes, of collecting so much data that the method of interpolation has little effect on the result, or of constructing a mathematical model that accurately represents the natural spatial variations in net accumulation with the minimum of parameterisation and calibration, are unfortunately still impractical.

The most obvious gaps in the data are those on Alexander Island and Wilkins Ice Shelf, and in south eastern Palmer Land. There is also major uncertainty in the areas that are ice-free in summer or where mean annual temperature is above -11°C and significant melting may occur. My treatment of ablation is certainly crude, but as the temperature database in the region is little better than the mass balance

database, the required parameterisations for a better treatment may not yet be possible (Morris and Vaughan, this report). Since the strong connection between temperature and mass balance means that ablation will be an important component of any response to climate change, the database for surface temperature is surely in just as much need of improvement as that for mass balance.

When the existing and any new data become available in a easily synthesised and manipulated form, i.e. a geographical information system (GIS), the task of identifying drainage basins, grounding lines, ice divides and boundaries between different climatic regimes will be infinitely simpler. The integration performed here uses, for the most part, a simple linear regression with altitude. With an improved and expanded dataset held in a GIS, a more sophisticated integration along the lines of Potter et al. (1984) would be worthwhile. Perhaps most importantly from the author's point of view, it could also be automated and quickly updated.

Finally, Jacobs et al. (in press) find a total net balance for the Antarctic Ice Sheet (all ice surfaces) of -469 Gt a^{-1} . As this deficit is roughly equal to the current total surface balance over the Antarctic Peninsula region, it would seem unwise to ignore the latter in future assessments of the state of the Antarctic Ice Sheet.

9. References

- Doake, C S M (1984). (R Frolich, personal communication) In: *Glaciological evidence: Antarctic Peninsula, Weddell Sea. in Glaciers, Ice Sheets and Sea Level: Effects of a CO₂-induced Climatic Change*. Rep. of a Workshop, Seattle, Sept. 13-15, 1984, National Academic Press, Wash. D.C. [also Dept. of Energy DOE/ER/60235-1], p. 197-209.
- Doake, C S M and Vaughan, D G (1991). Rapid disintegration of the Wordie Ice Shelf in response to atmospheric warming. *Nature*, **350**, p. 328-330.
- Giovinetto, M B and Bentley, C R (1985). Surface balance in ice drainage systems of Antarctica. *Antarctic Journal of the United States*, **20**(4), p. 6-13.
- Jacobs, S S, Hellmer, H H, Doake, C S M, Jenkins, A and Frolich, R M (in press). Melting of ice shelves and the mass balance of Antarctica. *Journal of Glaciology*.
- Jones, P D and Limbert, D W S, (1987). A data bank of Antarctic surface temperature and pressure data. *United States Department of Energy DOE/ER/60937-H2*.

Mercer, J H (1978). West Antarctic Ice Sheet and CO₂ greenhouse effect: a threat of disaster? *Nature* **271**, p. 321-325.

Morrison, S J (1990). Warmest year on record on the Antarctic Peninsula? *Weather* **45**, p. 231-232.

Paterson, W S B (1981). *The Physics of glaciers* (2nd edition), Oxford, Pergamon Press, p. 43-46.

Peel, D A and Clausen, H B (1982). Oxygen-isotope and total beta-radioactivity measurements on 10 m ice cores from the Antarctic Peninsula. *Journal of Glaciology*, **28**, p. 43-55.

Potter, J R, Paren, J G and Loynes, J (1984). Glaciological and oceanographic calculations of the mass balance and oxygen isotope ratio of a melting ice shelf. *Journal of Glaciology*, **30**, p. 161-170.

Reynolds, J M (1981). The distribution of mean annual temperatures in the Antarctic Peninsula. *British Antarctic Survey Bulletin*, **54**, p. 123-133.

Vaughan, D G, Mantripp, D R, Sievers, J and Doake, C S M (in press). A synthesis of remote sensing data on Wilkins Ice Shelf, Antarctica. *Annals of Glaciology*.

SPATIAL TEMPERATURE AND ACCUMULATION RATE VARIATIONS IN THE ANTARCTIC PENINSULA

David A Peel
British Antarctic Survey
Natural Environment Research Council
High Cross, Madingley Road
Cambridge, CB3 0ET
United Kingdom

Abstract

Current spatial trends in accumulation rate and temperature in the Antarctic Peninsula have been investigated using data obtained from shallow cores. Provisional algorithms linking accumulation rate with temperature and altitude have been computed for each of three zones which exhibit markedly different characteristics. Generally, it seems that snow accumulation rate closely parallels the mean saturation mixing ratio of water vapour, in line with similar behaviour over the continental ice sheet. Accumulation rates at several sites have increased by around 20% since about 1950, in parallel with a typically 1.9°C warming (at Faraday) since 1903, although this increase lies within the range of natural periodic fluctuations.

1. Scope of investigation

This investigation is concerned with factors affecting the short-term reaction of the surface of the ice cover to shifts in climate. The over-riding factor in the mass balance of the ice cover of the Antarctic ice sheet, and the major factor in the net mass balance of the Antarctic Peninsula sector, is the annual rate of net snow accumulation (snowfall \pm drift + condensation etc). This investigation will aim to identify and parameterize the principal thermodynamic and geographic controls on snow accumulation rate in the Peninsula, as a contribution towards predicting how the ice balance of the region might be perturbed by climate change.

Our investigation is confined to 98% of the area of the Peninsula region covered by the CEC Project, where the air temperature is below -11° . In these areas there is no run-off of summer meltwater and any summer melt is contained within the previous winter snow accumulation. Under such circumstances net accumulation measurements measured at stakes (and corrected for densification) will essentially record the same accumulation parameter as a core; except that the annual stratigraphic horizons along a core will not be coincident with calendar dates and derived accumulation rates must be averaged over several years to reduce this error. Moreover, these measurements will be more directly comparable with snow accumulation measurements across the Antarctic ice sheet, where ablation effects (apart from sublimation) can be neglected. The data are therefore

likely to be useful for studying the problem of changing mass balance arising from changing snow precipitation rates linked to shifts in water vapour content and transport of air masses advecting across the continent. Snowfall rate rather than net accumulation is also likely to be more amenable to interpretation by the climate modelling community.

A further reason for setting an upper limit of -11°C on the mean annual temperature of sites to be considered, is that mean annual air temperatures recorded at these sites, as inferred from the temperatures at 10 m depth, will not have been significantly raised by refreezing of percolating meltwater. Hence the primary influence of mean annual air temperature on accumulation rate can be investigated with minimal complications from secondary processes.

Our investigation will follow the following stages:

(i) Compilation of available 10 m temperature (T) data and accumulation (a) data derived mainly from pits and shallow (~ 10 m) cores.

(ii) Investigation of present-day spatial trends in accumulation rate and temperature, and their interrelationships. This will include short-scale depositional variability as well as regional variations - leading to parameterization of this behaviour to enable empirical predictions.

(iii) Investigation of temporal trends in accumulation

rate through the past century from deeper cores to establish the context for recent changes and to test whether relationships derived in (ii) are also applicable to time-trends.

(iv) Elucidation of some of the processes influencing temporal variations in accumulation rate in the Antarctic Peninsula.

Progress to-date relates mainly to parts (i) and (ii).

2. Sources of evidence on accumulation rate and temperature

Data have been compiled from sites (mean annual $T < -11^{\circ}\text{C}$) where 10 m cores have been collected. Figure 1 shows the distribution of sites where both T and a are available, where T alone is available, and where time series of a from deeper cores are available.

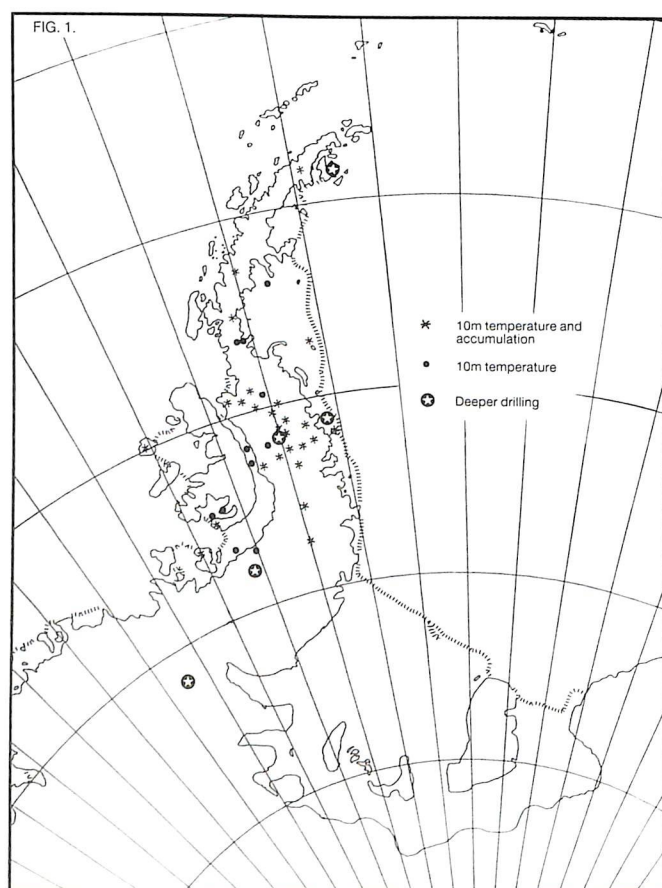


Figure 1. Distribution of sampling sites for 10 m temperatures and snow accumulation rate.

Accumulation rates have been estimated from the seasonal stable isotope stratigraphy, often supported by total β radioactivity measurements. Density profiles were measured at most of the sites. In general, sites on the east coast and on the plateau from around 70°S southwards can be dated accurately by stable isotope

analysis alone, whereas sites strongly influenced by cyclonic activity from the west often exhibit a more complex stratigraphy (Peel and Clausen, 1982). The deeper drilling sites are in general supported by extensive survey stake networks which reveal the statistics of local accumulation rate variations.

The decision to use core information only was made:

(i) to overcome potential problems in interpretation of occasional stake data available from several sites where the effects of settling for example, had not been fully taken into account

(ii) to avoid problems of frequently misleading interpretations of shallow pit stratigraphy.

The resulting data set should therefore be as homogeneous as possible, and give the best opportunity to characterize real spatial variations, rather than measurement noise.

The distribution of sampling sites is highly inhomogeneous, with a concentration of sites around the central region, extending to both the east and the west coasts, and a reasonable spread of sites along the axis of the Peninsula. The west coast region, and especially Alexander Island is grossly under-sampled, and the east coast only lightly sampled.

3. Present-day spatial relationships

Martin and Peel (1978) and Reynolds (1981) have examined the spatial and altitudinal controls on the distribution of 10 m temperatures in the Antarctic Peninsula region. Both papers showed that it was justifiable both statistically and climatologically to divide the Peninsula temperature data into west-central and east coast region sets. Eastwards of a line lying parallel to the topographic axis of the Peninsula at an altitude of around 1000 m, mean annual air temperatures, reduced to sea level, are around 6°C colder than in the central and western areas, although similar vertical lapse rates apply ($-0.57^{\circ}\text{C}/100\text{ m}$). Whilst the western and central areas are considered to have a maritime cyclonic climate, the east coast has a pseudo-continental climate dominated by extensive ice cover over the Weddell Sea (Schwerdtfeger, 1984). Statistically, both temperature data sets can be described fully on the basis of multiple linear regressions of temperature with altitude and latitude.

Snow accumulation rates averaged over the 3-30 years sampled by a 10 m core, are plotted in Figure 2a-c. No attempt has been made at this stage to normalise these data to a common time frame. In order to highlight some of the controlling factors, accumulation is plotted as a function of longitude,

temperature and altitude. The data point for Detroit Plateau is a clear outlier on all the plots (but plotted only on graph 2a) and should be regarded as erroneous. The dating at this site was highly tenuous, because due to excessive snow reworking along this exposed section of the Plateau, there was no clear stratification of the snowfall in either the visible or the isotope stratigraphy.

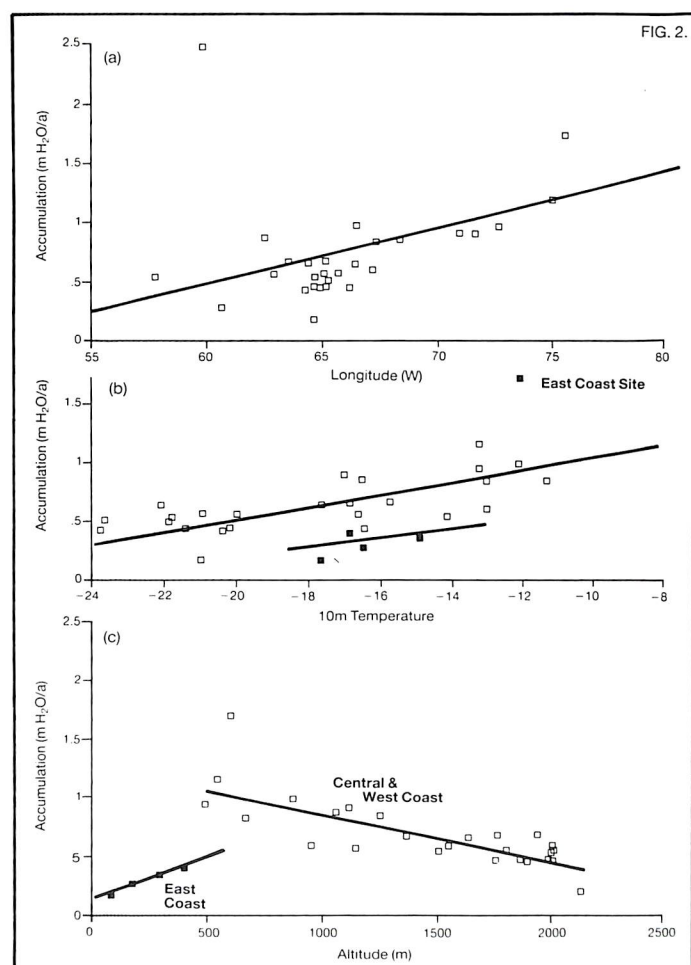


Figure 2. Mean annual snow accumulation rate in the Antarctic Peninsula as a function of longitude (2a), 10 m temperature (2b) and altitude (2c).

Figure 2a shows the marked two to three-fold increase in accumulation rate with progression from east to west

across the axis of the Peninsula. This reflects the shift from influence by cold, stably-stratified continental air on the east to air masses conditioned by cyclones tracking across open ocean to the west. This effect is more clearly seen in Figure 2b, where accumulation is plotted against mean air temperature. The East coast sites form a group with accumulation rates systematically around 50% lower than values for the West coast and central areas at the same temperature. For both the east and the west-coast groups the relative gradient of accumulation rate with temperature is very close to that of the saturation mixing ratio. The average gradient between -10°C and -24°C at 1000 mbar over water, is $3.44 / ^{\circ}\text{C}$ compared with the observed ratio of snow accumulation rates of $3.4 / ^{\circ}\text{C}$. This suggests that the broad approach used by Robin (1977) can be extended into the Antarctic Peninsula region. Robin demonstrated that the close relationship between snow accumulation across the Antarctic ice sheet and air temperature parallels closely the behaviour of the atmospheric saturation vapour pressure above the inversion layer. For parameterisation of accumulation rate in the Antarctic Peninsula it is clear that different equations, albeit with similar gradient, should be used to describe sites on the east coast and west/central areas respectively.

Figure 2c, the relationship with altitude, clearly separates a distinctive pattern of behaviour in three zones of the region. The central areas of the Peninsula show a strong linear trend with little scatter that has a gradient matching the mixing ratio line. Two of the three low-altitude west-coast sites fit the same relationship, but the third, on Charcot Island, exhibits an anomalously high value. This may reflect the close proximity of this site to open ocean, or be due to problems of interpreting the isotopic stratigraphy at a high accumulation site. Clearly, more data are needed from a wider altitude range on Alexander Island in order to improve parameterization of this zone. Finally, the east-coast sites show evidence for an inverse gradient of accumulation with elevation, albeit over a narrow altitude band (130-400 m). This may be related to a high frequency of stable temperature inversions over the Weddell Sea zone.

ZONE	Present Accumulation rate (mean) m water/a	Coefficients of regression with Alt (m) and T ($^{\circ}\text{C}$)
West Coast	1.26 ± 0.39	$1.32 - 0.000449 Alt$ ($r = -0.79$)
Central	0.61 ± 0.16	$1.56 + 0.0508 T$ ($r = 0.66$)
East Coast	0.31 ± 0.08	$0.149 + 0.00064 Alt$ ($r = 0.97$) $0.904 + 0.036 T$ ($r = 0.52$)

Table 1. Provisional algorithms for accumulation rate variations in the Antarctic Peninsula

Provisional algorithms for estimating the present-day spatial distribution of accumulation rate in the three zones are given in Table 1. The present-day temperature sensitivity is also given, although application of these gradients to the prediction of accumulation rate changes in response to climatic shifts is premature.

4. Longer term trends

Figure 3 is a compilation of trends in accumulation rate during the past century derived from deeper cores drilled in the region.

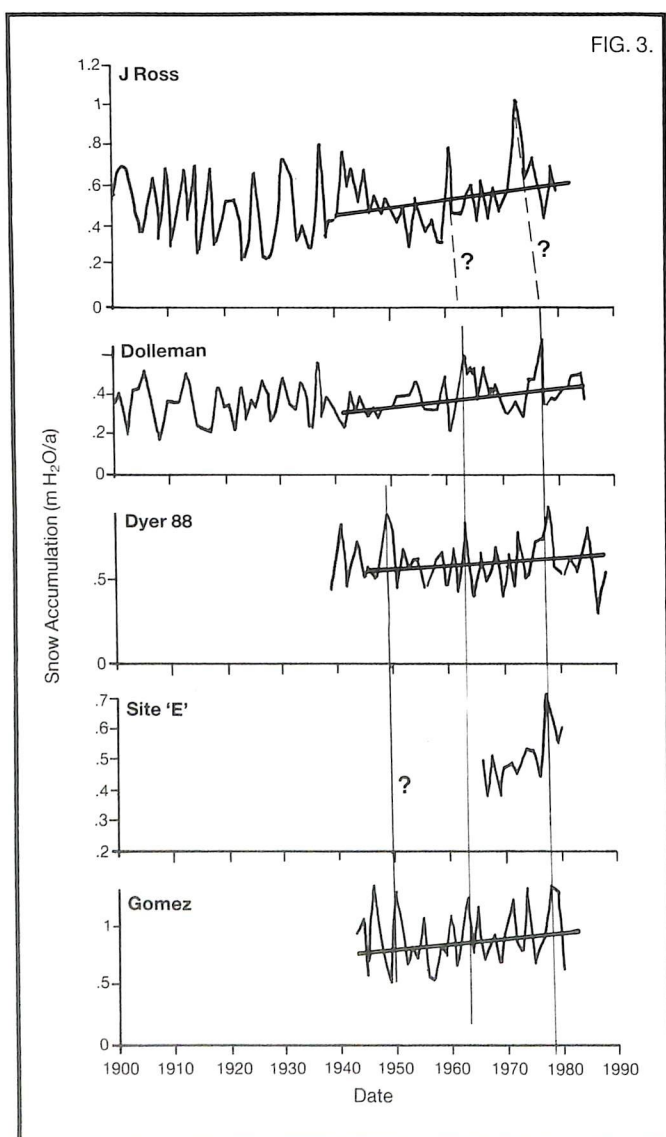


Figure 3. Time-trends in annual snow accumulation rate in the Antarctic Peninsula derived from ice cores.

The data for James Ross Island are taken from Aristarain and Jouzel (1986), and have been subjected

to a small first-order correction for thinning assuming uniform vertical strain-rate. In all cases there is evidence for an increase of around 20% in accumulation rate since about 1950. The increase however, lies within the range of large, natural periodic fluctuations although clearly it is a regional feature, extending from 64°S to 74°S and including both the central and east coast zones. Levels around 1950 fell below the longer term average, tending to over-emphasise the recent increase, which is however comparable with the relative increase in mixing ratio of ~17% expected on the basis of a 1.9°C warming computed for Faraday since 1903 (Jones et al., in press).

5. Future work

New data are needed from certain key areas of the Peninsula in order to improve the spatial parameterization of snow accumulation rates. Of most significance is the E/W and altitudinal character of accumulation variations across Alexander Island and adjacent areas.

In order to minimise "experimental scatter" in the data set, arising from the irregular sampling dates and time-averaging, the data should be normalised to a common time-frame on the basis of a best-estimate of the regionally-representative accumulation time-series. To extend the spatial representation of the accumulation time series, use will be made of precipitation 'proxies' based on the recorded frequency of snowfall observations at Faraday, Rothera, Signy and Halley.

The ultimate aim is to achieve the most authoritative statement on the nature and long-term significance of accumulation rate variations in the Antarctic Peninsula region. This will include an examination of processes responsible for changing accumulation rate, to provide a physical basis for the derived empirical accumulation/T relationships and hence increase confidence in projecting these relationships forwards.

6. References

- Aristarain, A J, J Jouzel and M Pourchet (1986). Past Antarctic Peninsula Climate (1850-1980) deduced from an ice core isotope record. *Climatic Record*, **8**, p. 69-89.
- Jones, P D, R Marsh, T M L Wigley, and D A Peel (in press). Decadal Timescale Links between Antarctic Peninsula Ice Core Oxygen-18, Deuterium and Temperature. *The Holocene*.

Martin, P J and D A Peel (1978). The spatial distribution of 10 m temperatures in the Antarctic Peninsula, *Journal of Glaciology*, **20**, No. 83, p. 311-17.

Peel, D A and H B Clausen (1982). Oxygen-isotope and total beta-radioactivity measurements on 10 m ice cores from the Antarctic Peninsula. *Journal of Glaciology*, **28**, No. 98, p. 43-45.

Reynolds, J M (1981). The Distribution of Mean Annual Temperatures in the Antarctic Peninsula. *British Antarctic Survey Bulletin*, **54**, p. 123-133.

Robin, G de Q (1977). Ice cores and climatic change. *Philosophical Transactions of the Royal Society of London*, Ser B. **280**, No. 972, p. 143-68.

Schwerdtfeger, W (1984). Developments in Atmospheric Science. *Weather and Climate of the Antarctic* **15**, Amsterdam, Elsevier.

SNOW SURFACE TEMPERATURES IN WEST ANTARCTICA

E M Morris and D G Vaughan
British Antarctic Survey
Natural Environment Research Council
High Cross, Madingley Road
Cambridge, CB3 0ET
United Kingdom

Abstract

Snow temperatures measured at around 10 m depth over the period 1957 to 1992 have been used to derive a map of mean annual surface temperature over the Antarctic Peninsula and Filchner-Ronne Ice Shelf. Linear regression analysis has been used to calculate lapse rates west and east of the topographic divide running along the spine of the Antarctic Peninsula. There is evidence of climatic warming on the Filchner-Ronne Ice Shelf, but elsewhere temporal variability obscures any warming trend.

1. Introduction

In areas where there are no meteorological records the mean annual air temperature at the snow surface is commonly estimated by assuming that it is the same as the snow temperature measured at a depth of 10 m. The accuracy of this estimate depends on (i) the structure of the snow (ii) the pattern of air temperature variation within the year and (iii) whether there is any long term temperature change. Maps of snow surface temperature in West Antarctica have been published by Shimizu (1964), Thomas (1976), Martin and Peel (1978) and Reynolds (1981). They are based on borehole measurements, not all taken at 10 m depth, made at different times of the year and over a period of some thirty years. Although the spatial temperature distribution over the continent has been reasonably well-established by these authors the accuracy of the surface temperature estimates is not sufficient to allow detection of temporal change. Raper et al. (1984) have produced an areally weighted Antarctic surface temperature time series for the period 1957-82 using air temperature measurements. The annual average time series shows a warming of $0.029^{\circ}\text{C a}^{-1}$ i.e. an increase of 0.9°C over 30 years. This is comparable to the uncertainty in the estimates of surface temperature derived by previous authors from borehole data. It is the purpose of this paper to present an updated map for the Antarctic Peninsula and the Filchner-Ronne Ice Shelf using a more precise method for determining mean annual surface temperature from borehole data (Morris, 1991) and to examine whether there is any evidence of long-term change over the region.

2. Derivation of surface temperatures

It is assumed that the accumulation, densification and metamorphosis of polar snow is controlled by the local climate in such a way that the snow cover at sites with the same surface temperature history, $T_s(t)$, will develop broadly the same physical properties. In particular, it is supposed that the variation of thermal diffusivity in the upper 10 m of snow will be similar for sites of similar $T_s(t)$. In this case a standard set of snow temperature curves $T(d,t)$ will apply for all sites with the same surface temperature history. The temperature in a borehole at depth d and time t may be written

$$T(d, t) = T_m + a F(T_s, d, t) \quad (1)$$

where T_m is the mean annual surface temperature and a is the amplitude of the first harmonic of the annual temperature wave at the surface. If F can be estimated for a given site a borehole temperature profile measured at a given time can be used to determine both T_m and a . If the snow temperature has only been measured at one depth, both F and a must be estimated to determine T_m .

2.1 Meteorological data from the Antarctic

T_m is known and an estimate of amplitude a can be made at sites where air temperature is recorded throughout the year. Table 1 lists the meteorological observing stations in the West Antarctic area south of 62°S and between 10°W and 110°W . (Plateau Station has also been included in Table 1 for convenience).

Station	Lat/°S	Long/°W	Alt/m	T_a /°C	a /°C	Date
Eduardo Frei	62.25	58.93	10	-2.4	4	1970-84
Bellingshausen	62.20	58.93	16	-2.9	4	1947-84
Arturo Prat	62.50	59.68	5	-2.7	4	1966-84
Esperanza	63.40	56.98	8	-5.8	6	1953-77
Bernardo O'Higgins	63.32	57.90	10	-4.2	4	1963-76
Marambio	64.23	56.72	198	-9.1	7	1971-83
Admiralty Bay	62.05	58.40	19	-2.4		1970-78
Deception	62.98	60.57	8	-2.6		1970-78
Hope Bay	62.40	56.98	11	-5.59		1970-78
Palmer Station	64.77	64.08	20	-3.2		1974-80
Faraday	65.25	64.27	10	-3.54	5	1970-78
Rothera	67.57	68.13	20	-6.36	7	1977-86
Adelaide	67.77	68.92	14	-4.7		1970-80
Fossil Bluff	71.33	68.28	55	-11.1	11	1968
Halley	75.52	26.62	29	-18.19	10	1970-80
Eights	75.30	77.12	450	-25.9		1964-65
Ellsworth	77.72	41.12	43	-23.4		1957-58
Siple Station	75.93	84.25	1054	-25.5	12	1982-83
Plateau	79.30	-40.50	3624	-59.8	18	1967-68
Amundsen-Scott	90.00	0.00	2800	-49.3	18	1957-85
Byrd	80.02	119.53	1515	-28.1	10	1957-69
Maudheim	71.05	10.93	37	-17.61	11	1950-51

Table 1. Meteorological Observing Stations.

These stations record or have recorded screen temperature at a fixed height, nominally 1.5 m, above the snow surface. For temperatures warmer than -40°C the mean annual screen temperature should be within 0.5°C of the mean annual surface air temperature (Loewe, 1970). The average mean annual temperature and the estimate of amplitude a have been determined from the tables of monthly mean temperatures given by Jones and Limbert (1989) or are given by Macdowell (1964), Dalrymple et al. (1966), Loewe (1970), Sanderson (1978) and Reynolds (1981). Table 2 shows Automatic Weather Stations (Stearns and Weidner, 1990) in the same area which record air temperature at a nominal height of 3 m which decreases as the station is buried by snow. The mean annual temperature and amplitude a for an example year (1989) have been estimated from tables of monthly mean temperatures given by Keller et al. (1990).

Figure 1 shows the departures of monthly mean screen temperature from the annual mean (T_a) for some example stations. The more southerly stations show an asymmetrical variation, the so-called "coreless" winter. A key to this behaviour is given by an examination of solar radiation, which has a major influence on air temperature. Between the South Pole and the Antarctic Circle the annual variation of insolation is a truncated sinusoidal curve with a flat section of zero insolation during the winter. The insolation curve can be described by the sum of two Fourier components with amplitudes A_1 and A_2 . The ratio A_2/A_1 varies from 0 at the Antarctic Circle to 0.42 at the Pole. As it increases so the typical polar annual variation curve develops with a flattened broad region in the winter and a strong narrow peak in the summer.

Site	Lat/°S	Long/°W	Alt/m	T_a /°C	a /°C	Date
Uranus Glacier	71.43	68.93	780	-10.9	7	1989
Cape Adams	75.00	62.50	25	-21	8	1989
Larsen Ice	66.97	60.55	17	-12	5	1989
Siple Station	75.90	83.92	1054	-24.3	10	1989

Table 2. Automatic Weather Stations.

The amplitude of the first harmonic of the annual temperature wave varies from about 4°C at the northern end of the Antarctic Peninsula to 18°C at the pole. In the south part of the peninsula and on the Filchner-Ronne Ice Shelf a is around 11°C.

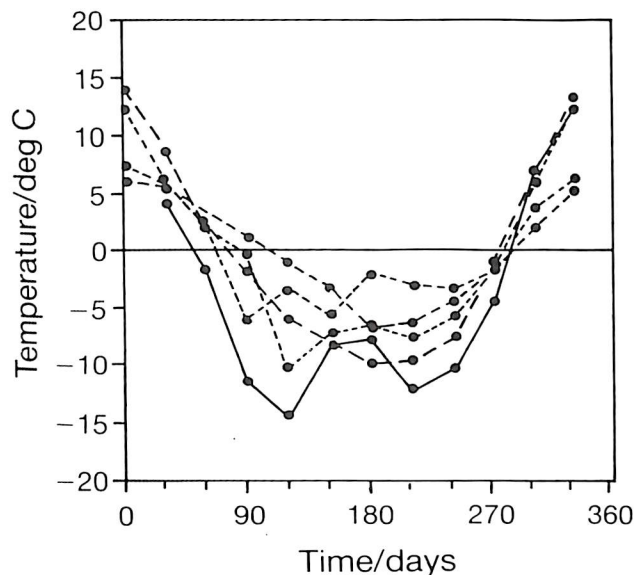


Figure 1. Deviation of the monthly mean air temperature from the annual mean for Cape Adams Automatic Weather Station (solid line), and Halley, Rothera, the Uranus Glacier AWS and Siple (decreasing length of dash).

2.2 Measured snow temperature variations

The function F is known at sites where snow temperatures have been measured at different depths throughout the year. Data from Halley Bay (Maddowell, 1964), South Pole Station (Dalrymple et al., 1966) Plateau Station (Weller and Schwerdtfeger, 1977) and Maudheim (Dalrymple et al., 1966) are shown in Figure 2. The temperatures are shown as deviations from the mean annual surface temperature normalised by the amplitude of the first harmonic of the annual temperature wave at the surface, i.e. the function plotted is F as defined in equation (1). The shape of the curve varies with latitude. The Maudheim and Halley curves are similar (Figure 2a) while a considerable difference is apparent between the Maudheim and South Pole curves (Figure 2b).

2.3 The nomogram

For sites in the Antarctic Peninsula and on the Filchner-Ronne Ice Shelf where snow temperatures have not been measured it is suggested that F can be estimated by using Figure 2c as a nomogram (Morris and Vaughan, 1991). For a given day the value of F at a given depth can be determined by interpolation between the Plateau Station or the Maudheim curves.

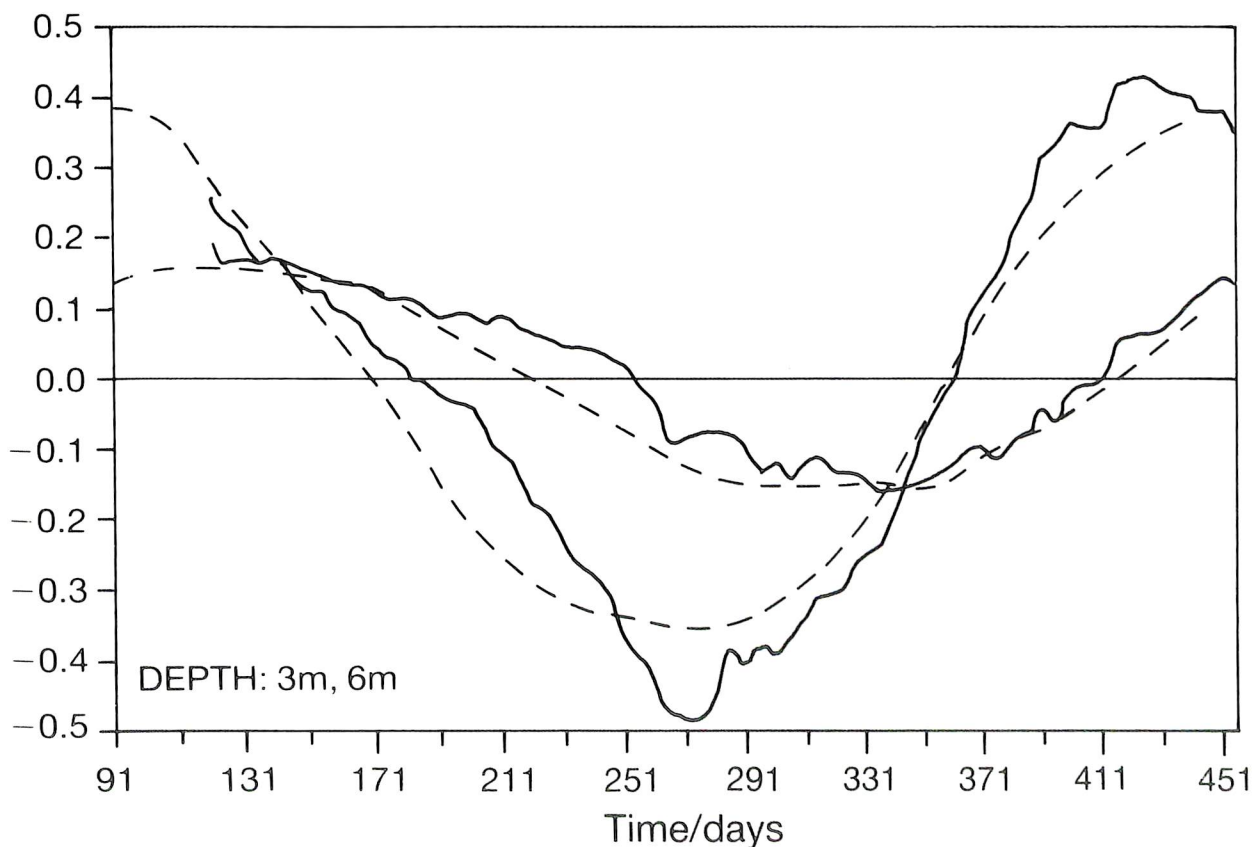


Figure 2(a). Snow temperatures (decreasing with depth) measured at Maudheim (dashed line) and Halley Bay (solid line).

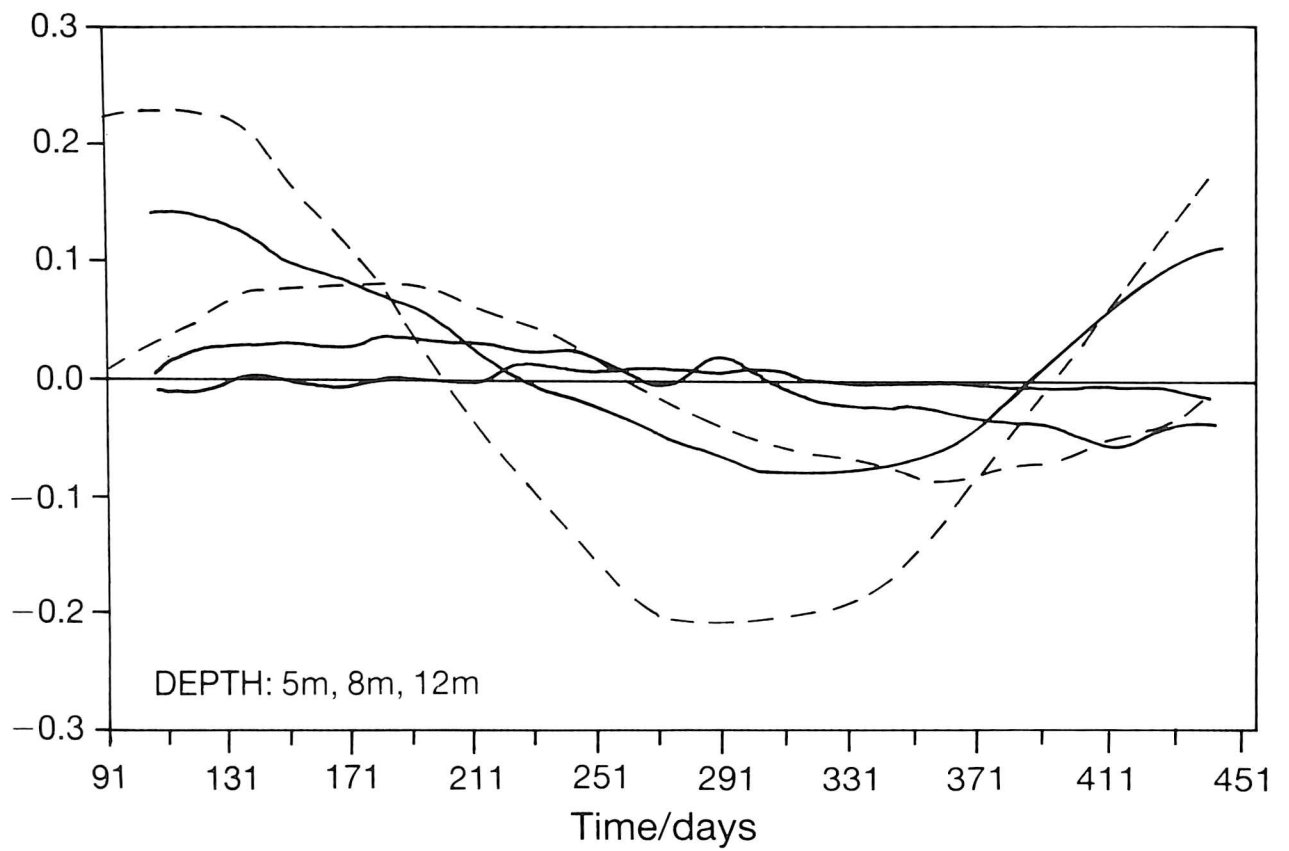


Figure 2(b). Snow temperatures (decreasing with depth) measured at Maudheim (dashed line) and South Pole Station (later Amundsen-Scott Station. Solid line).

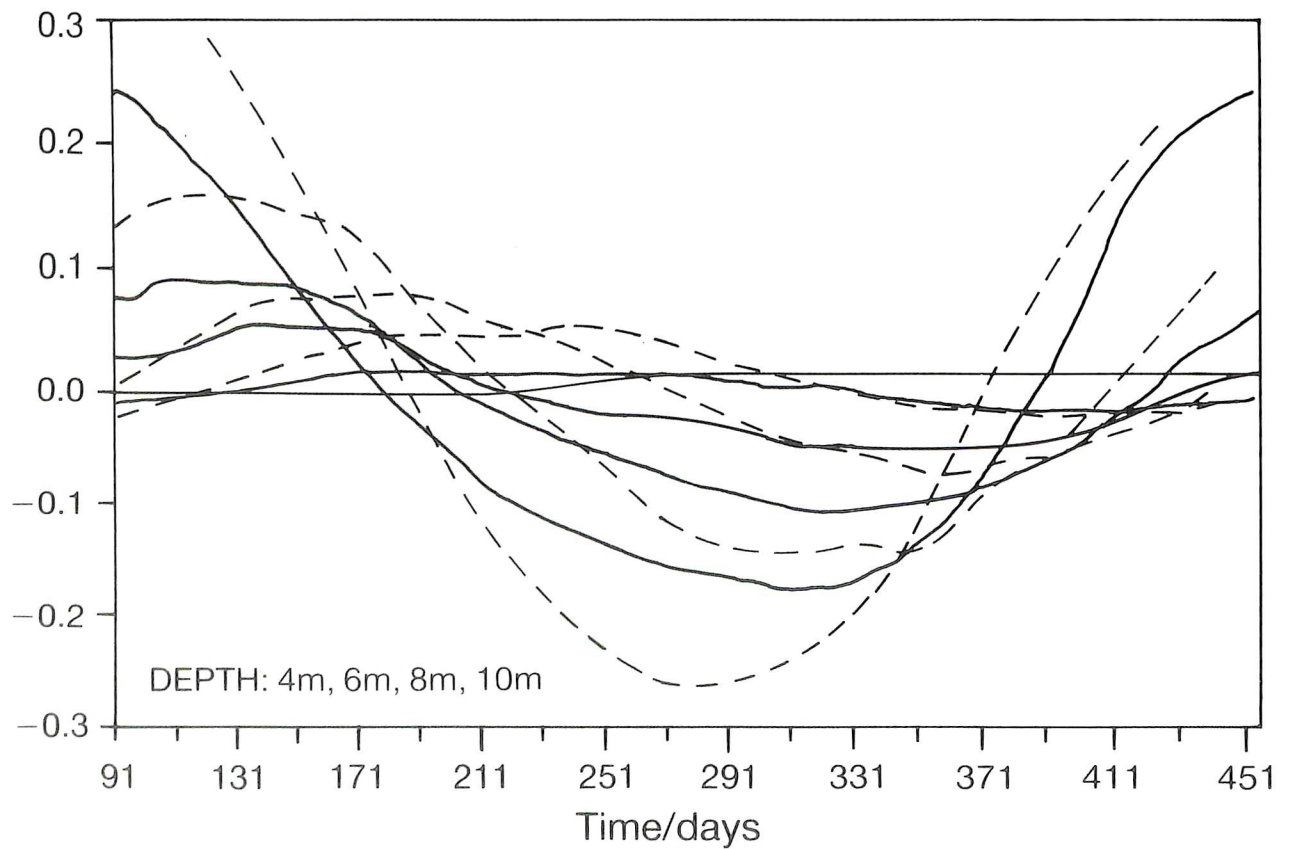


Figure 2(c). Snow temperatures (decreasing with depth) measured at Maudheim (dashed line) and Plateau Station (solid line).

For sites on the Filchner-Ronne Ice Shelf and in Ellsworth Land the best estimate of F at the moment is given by the Plateau Station data although snow temperature variations are being recorded at a site on the ice shelf and may be available in 1993 (Nicholls, pers. comm.). In Palmer Land the Maudheim curves give a better estimate of F . Note that as soon as the summer air temperatures rise above the melting point the shape of the snow temperature curves will change substantially, so the Maudheim curves cannot be applied when the mean annual temperature is warmer than around -11°C .

3. Data from boreholes

A database of borehole temperature data for the Antarctic Peninsula and Filchner-Ronne Ice Shelf is being compiled at BAS under the auspices of the international Filchner-Ronne Ice Shelf Programme (FRISP). Figure 3 shows the sites for which data have been obtained. So far 238 measurements covering the period 1957-92 have been extracted from published and unpublished sources but there are undoubtedly further data to be found, especially from Argentinian and Chilean sources.

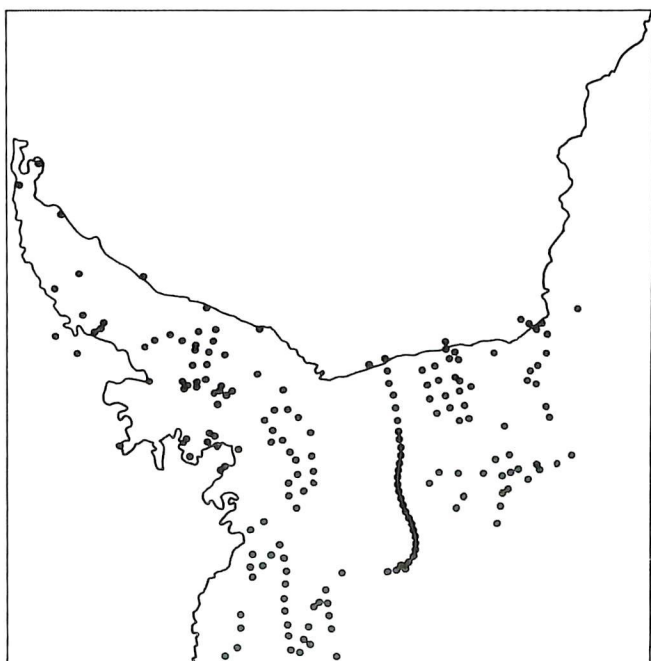


Figure 3. Sites at which borehole temperatures have been measured. The generalised coast line is schematic only and does not show Adelaide Island.

3.1 Ellsworth Traverses 1957-58, 1958-59

Early snow temperature measurements on the Filchner-Ronne Ice Shelf were made by US parties (Aughenbaugh et al., 1958; Godwin, 1959) using a Leeds and Northrup thermohm left in the borehole for at least 2 hours. The depth of the borehole (usually not 10 m) is given explicitly in the record of the US data, as is the date of the measurement, so it is possible to calculate T_m from the measured $T(d,t)$ using the appropriate value of F from the nomogram and an estimated value for a of 11°C . Corrections of up to 0.5°C are required for some of the data from shallow boreholes.

3.2 Ellsworth Highland Traverse 1960-61

This traverse covered 1215 nautical miles from Byrd Station to Camp Minnesota. Every 24 miles a 2 m or 3 m pit was dug and a core taken from the bottom of the pit to 10 m below the surface. The 10 m temperature was again measured by a Leeds and Northrup thermohm set in the drill hole for at least 2 hours. The exact depth of the borehole is not recorded in the published paper (Shimizu, 1964) so for the moment it has been taken to be the nominal value of 10 m. T_m has been calculated using $a = 13^{\circ}\text{C}$ and is usually about 0.3°C warmer than the 10 m temperature.

3.3 Antarctic Peninsula Traverse 1961-62

The same methods were used the following year (Shimizu, 1964) on a traverse of 1052 statute miles from Camp Minnesota to Ski-Hi. Again the exact depth of the borehole is not available so has been taken to be 10 m exactly except at Ski-Hi and mile 796 station where the depths are taken as 21 m and 25 m respectively. Except for those deeper boreholes T_m calculated using $a = 13^{\circ}\text{C}$ is about 0.3°C warmer than the borehole temperature.

3.4 GAP network 1971-1992

As part of the Glaciology of the Antarctic Peninsula programme (GAP) a series of borehole temperature measurements were made by British Antarctic Survey scientists. Most of the boreholes were drilled to a nominal 10 m and the temperature measured at the bottom of the borehole after a thermocouple and/or a lagged thermometer had been left overnight. Most of these temperatures have been published by Martin and Peel (1978) and Reynolds (1981). It has been possible to go back to field note books held in the archives of BAS to determine the exact depth and date of each temperature measurement. As a bonus some glaciologists (notably J F Bishop and J G Paren) made careful measurements of temperature profiles after the

sensor had been left for 12-24 hours in the borehole and using these data it is possible to check the validity of the nomogram for *F*.

3.5 Filchner Network 1984-1992

A network of measurements have been made on the Filchner-Ronne Ice Shelf south of Filchner Station by a series of German parties (not necessarily using the same instruments or measurement techniques) and a British group (Reinwarth et al., 1985; Bamber, pers. comm.). We have assumed, pending further information, that the German temperatures were all measured at 10 m and have estimated mean annual temperature accordingly. The most recent British measurements are fully documented, and were made using a thermistor.

3.6 Rutford Flowline 1986-87

Temperatures along a flow line running from the Rutford Ice Stream to the Ronne ice front are reported by Jenkins (1986, 1987, 1988). These were all measured exactly at 10 m using a lagged thermometer and have been corrected using $a = 13^\circ\text{C}$.

3.7 South Ronne Traverse 1990-91

Borehole temperature measurements on the South Ronne Ice Shelf were made by Morris (1991) using a thermistor at depths between 7.4 m and 8.9 m. At two sites a German party repeated the measurement a year later (Oerter et al., 1990).

4. Analysis

Regression analysis using all data for which the time of observation is known (205 observations) produces lapse rates as shown in the first line of Table 3. The altitudinal lapse rate is $-(0.0057 \pm 0.0005)^\circ\text{C m}^{-1}$. Mean annual surface temperatures corrected to sea level using this lapse rate are plotted in Figure 4. The contours are at 2.5°C intervals from -25°C to -7.5°C .

Mean annual temperature decreases with increasing latitude, as expected, and the east side of the Antarctic Peninsula is clearly colder than the west side as established by Martin and Peel (1978). Morris and Vaughan (1991) have established that because of the strong winter inversion in the Filchner-Ronne Ice Shelf region mean annual temperature increases with altitude by $0.005^\circ\text{C m}^{-1}$ up to about 700 m asl so there are warm spots over Berkner Island, Henry and Korff ice rises and the edge of the Plateau south of Berkner Island. Not all of these are resolved in Figure 4 but they may be seen in a more detailed map of temperatures over the Ronne-Filchner Ice Shelf in Morris (1991).

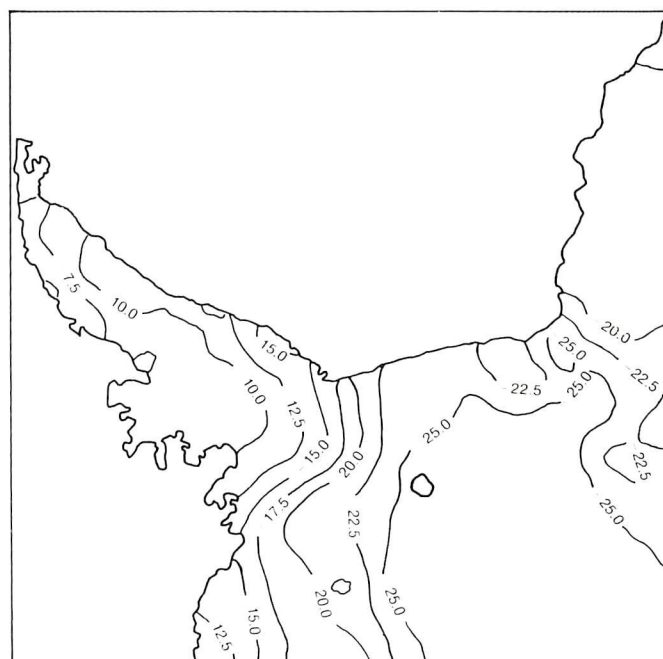


Figure 4. Mean annual surface temperature ($^\circ\text{C}$) corrected to sea level using a lapse rate of $0.006^\circ\text{C m}^{-1}$.

Data set	Latitudinal lapse rate $^\circ\text{C deg}^{-1}$	Longitudinal lapse rate $^\circ\text{C deg}^{-1}$	Altitudinal lapse rate $^\circ\text{C m}^{-1}$	Temporal lapse rate $^\circ\text{C a}^{-1}$	r^2	N
All sites	1.99 ± 0.08	0.002 ± 0.018	-0.0057 ± 0.0005	-0.045 ± 0.021	0.76	205
Western sites	1.12 ± 0.30	0.148 ± 0.074	-0.0082 ± 0.0006	0.040 ± 0.076	0.77	70
Eastern sites	1.05 ± 0.07	0.067 ± 0.008	0.00008 ± 0.00036	0.014 ± 0.009	0.81	135
Western sites north of 74°S	1.11 ± 0.33	0.098 ± 0.081	-0.0082 ± 0.0007	0.006 ± 0.088	0.75	59
Eastern sites above 700 masl	1.23 ± 0.16	0.115 ± 0.034	-0.0040 ± 0.0009	-0.015 ± 0.056	0.78	33
Eastern sites below 700 masl	0.99 ± 0.04	0.073 ± 0.008	0.0039 ± 0.0008	0.027 ± 0.008	0.89	102

Table 3. Lapse rates for mean annual surface temperature.

Figure 5 shows the variation of mean annual surface temperature (corrected to sea level as above) with latitude. The data collected east and west of the topographic divide running along the spine of the Antarctic Peninsula and into Ellsworth Land form two groups with lapse rates as shown in Table 3.

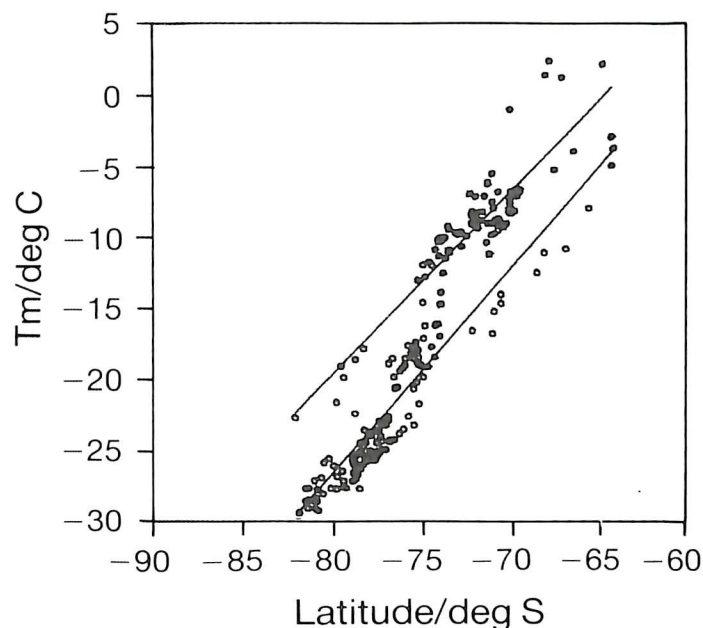


Figure 5. Variation of mean annual surface temperature corrected to sea level with latitude. Separate regression lines for east and west coast data are shown. West coast temperatures are higher than east coast temperatures.

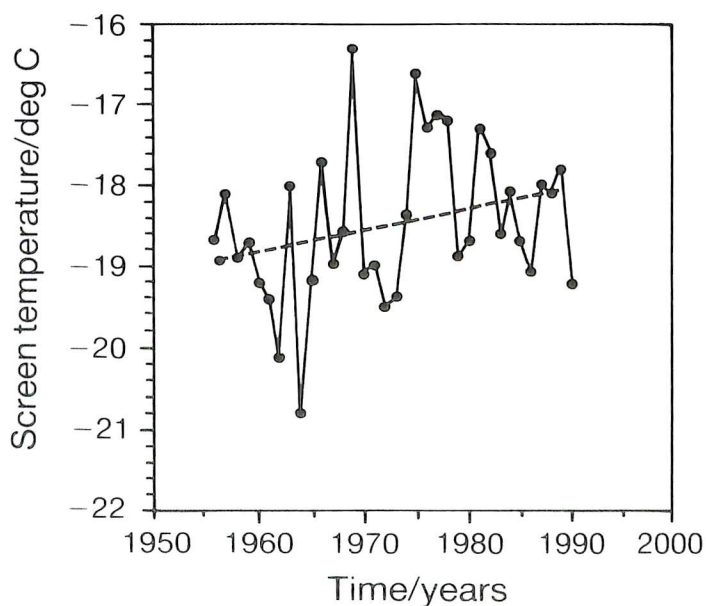


Figure 6. Mean annual screen temperature at Halley Station.

Separation of the data into western and eastern groups improves the fit but increases the uncertainty in the temporal lapse rate. A further separation into data taken north of 74°S on the west side of the Antarctic Peninsula itself, data east of the divide but above the inversion layer, and data collected on the Ronne-Filchner Ice Shelf produces improved fits and more logical altitudinal lapse rates. The results are not incompatible with the climatic warming of 0.029°C a⁻¹ suggested by Raper et al. (1984) but certainly do not demonstrate it. The difficulty lies of course in the large temporal variability of mean annual temperatures, illustrated in Figure 6 which shows mean annual screen temperature at Halley for 1956-1990. Over this period the temporal lapse rate is (0.027 ± 0.016)°C a⁻¹ with r² = 0.08. This is comparable to the lapse rate of (0.027 ± 0.008)°C a⁻¹ obtained for the eastern sites below 700 m asl.

Further work will be focused on deriving more sophisticated models for the spatial and temporal dependence of T_m to make better use of the current data set, and on the acquisition of new data in Alexander Island and the southern part of the Antarctic Peninsula. In particular it will be important to take into account the lag time between borehole temperatures and air temperatures when investigating the temporal variability.

Acknowledgements

We should like to thank D Mantripp, J Bamber, K W Nicholls, R Mulvaney and H Oerter for providing unpublished borehole temperature measurements.

References

- Aughenbaugh, N, H Neuberg and P Walker (1958). Ellsworth Station, Glaciological and Geological Data 1957-1958. In: *Report 825-1 Part I USNC-IGY Antarctic Glaciological Data. Field Work 1957 and 1958*. Ed. R P Goldthwait. The Ohio State University Research Foundation, Columbus, Ohio. p.1-158.
- Dalrymple, P C, H Lettau and H Wollaston (1966). South Pole micrometeorology program (data analysis). *Antarctic Research Series 9, Studies in Antarctic Meteorology*, ed: M J Rubin. American Geophysical Union, Washington, DC. p. 13-57
- Goodwin, R (1959). Part III. Ellsworth Traverse. *USNC-IGY Antarctic Glaciological Data. Report No. 2: Field Work 1958-59*. Submitted by R P Goldthwait. The Ohio State University Research Foundation, Columbus, Ohio. 80 pp.

- Jenkins, A J (1986). Glaciological Field Work on the Ronne Ice Shelf 1985/86. *BAS Field Report R/85-86/S3*.
- Jenkins, A J (1987). Glaciological Field Work on the Ronne Ice Shelf 1986/87. *BAS Field Report R/1986-87/S2*.
- Jenkins, A J (1988). Glaciological Field Work on the Ronne Ice Shelf 1987/88. *BAS Field Report R/1987-88/S2*.
- Jenkins, A J and C S M Doake (1991). Ice-Ocean Interaction on Ronne Ice Shelf, Antarctica. *Journal of Geophysical Research*, **96**, No. C1 p. 791-813.
- Jones, P D and D W S Limbert (1989). Antarctic surface pressure and temperature data. Oakridge National Laboratory Carbon Dioxide information Analysis Center, Environmental Sciences Division Publication No. 3215.
- Keller, L M, G A Weidner and C R Stearns (1990). Antarctic Automatic Weather Station Data for the calendar year 1989. Department of Meteorology, University of Wisconsin.
- Loewe, F (1970). Screen temperatures and 10 m temperatures. *Journal of Glaciology*, **9**, No. 56, p. 263-68.
- Maddowell, J (1964). Glaciological observations at the base. In: *The Royal Society International Geophysical Year Antarctic Expedition. Halley Bay. Coats land, Falkland Islands Dependencies. 1955-59*. London, The Royal Society 1964, Volume IV, p. 269-313.
- Martin, P J and D A Peel (1978). The spatial distribution of 10 m temperatures in the Antarctic Peninsula. *Journal of Glaciology*, **20**, No. 83 p. 311-317.
- Morris, E M (1991). Report of glaciological field work on the Ronne Ice Shelf. Sledge Quebec 1990/91. *BAS Field Report R/1990/S2*.
- Morris, E M and D G Vaughan (1991). Glaciological measurements on the South Ronne Ice Shelf. In: *Filchner-Ronne Ice Shelf Programme Report No. 5*. Eds. H Miller and H Oerter. p. 37-44.
- Oerter, H, J Kipfstuhl, H Miller, A Minikin, D Wagenbach, W Graf and O Reinwarth (1990). *Filchner Ronne Ice Shelf Programme Report No. 4*, Alfred-Wegener-Institute for Polar and Marine Research, Bremerhaven. p. 98-103.
- Raper, S C B, T M L Wigley, P R Mayes, P D Jones, and M J Salinger, (1984). Variations in surface air temperatures: Part 3. The Antarctic, 1957-1982. *Monthly Weather Review*, **112**, p. 1341-1353.
- Reinwarth, O, W Graf, W Stichler, H Moser and H Oerter (1985). Investigations of the Oxygen-18 content of samples from snowpits and ice cores from the Filchner Ronne Ice Shelves and Ekström Ice Shelf. *Annals of Glaciology*, **7**, p. 49-53.
- Reynolds, J M (1981). The distribution of mean annual temperatures in the Antarctic Peninsula. *BAS Bulletin*, **54**, p. 123-133.
- Sanderson, T J O (1978). Thermal stresses near the surface of a glacier. *Journal of Glaciology*, **20**, No. 83, p. 257-283.
- Stearns, C R and G A Weidner (1990). Antarctic Automatic Weather Stations: Austral summer 1989-90. *Antarctic Journal of the United States 1990 Review* Volume XXV, No. 5. p. 254-258.
- Shimizu, H (1964). Glaciological studies in West Antarctica, 1960-1962. In: *Antarctic Snow and Ice Studies*. Ed. M Mellor. *Antarctic Research Series*, Volume 2. AGU Publication No.1197. p. 37-64,
- Thomas, R H (1976). The distribution of 10 m temperatures on the Ross Ice Shelf. *Journal of Glaciology*, **16**, No. 74, p. 111-117.
- Weller, G and P Schwerdtfeger (1977). Thermal properties and heat transfer processes of low-temperature snow. In: *Meteorological Studies at Plateau Station, Antarctica*. Ed. J A Businger. *Antarctic Research Series*, AGU, Vol. 25, p. 27-34.

GLOBAL CLIMATE MODELS AND ANTARCTICA

William Connolley
British Antarctic Survey
Natural Environment Research Council
High Cross, Madingley Road
Cambridge, CB3 0ET
United Kingdom

Abstract

Global Circulation Models can be a powerful tool to investigate possible climate changes. Over data-sparse regions such as Antarctica, they may offer valuable information about the current climate. There are, however, many areas where models need to be improved, and in this paper I consider the representation of the oceans, sea ice and steep orography, which are particularly relevant to modelling around Antarctica.

1. Introduction

Global Climate Models (GCMs) can simulate the present climate with "considerable skill" (IPCC 1990). In Simmonds (1990) results from many models are compared and evidence is given of an increase in skill as models have become more sophisticated and their resolutions have become finer. Mitchell and Senior (1989) examined the performance of the United Kingdom Meteorological Office (UKMO) climate model over Antarctica in winter and found good agreement between surface pressure and temperature fields from the model and operational analyses. Simulations of the current climate can use climatological values for sea surface temperatures and sea ice extents, but GCMs attempting to predict climate change must include an ocean and a sea ice model. There are problems with both of these.

2. Oceans

Both atmosphere and ocean models have typical horizontal resolutions of 500 km. This will resolve most energetically-important scales of motion in the atmosphere, but the corresponding oceanic motions are on scales of less than 50 km. These scales cannot be resolved by today's models and to make them stable high values of artificial viscosity are required, which leads to sluggish oceanic motion. This in turn affects the atmosphere, as oceanic heat transport and temperatures are a vital influence on the atmosphere. To provide a realistic climate, a technique called flux correction is used, whereby the heat and salinity fluxes into the ocean required in a control to provide adequate simulation of these

variables are computed, and averages of these fluxes are fed into the climate change simulations. This assumes that the climate change being modelled is a small perturbation on the basic state, so that the calculated flux corrections remain valid. In a sense the flux corrections are playing the part of the missing oceanic circulation, since the flux corrections applied into the ocean are effectively transporting heat and salinity horizontally.

3. Sea Ice

Sea ice has a significant effect on the climate around Antarctica (King 1991 shows anti-correlations between sea ice extent and temperatures on the Antarctic Peninsula) because it acts as a barrier to heat and moisture exchange between the ocean and atmosphere, and because its high albedo acts to reflect incident radiation. It can also modify the momentum exchange between atmosphere and ocean. Sea ice is a complicated substance which can be modelled as having limited resistance to compression and no resistance to tension. Such a model (Hibler 1979) is generally too expensive to run in a GCM. Sea ice models used in GCMs are usually simpler and only model the formation of sea ice due to freezing, though some (e.g. the UKMO model) do include important effects such as brine rejection. They do not include movement of the ice, but the UKMO and others (e.g. NCAR) are currently considering a more sophisticated model which would include motion. Between austral summer and winter there is a 5-fold expansion of the sea ice around Antarctica, which implies that most of the winter ice is first-year ice. In the Arctic, the winter expansion is smaller and more of

the ice is multi-year. An important mechanism for the winter expansion around Antarctica is the advection northwards by the inversion winds which flow off the continent of the ice formed near the coasts. Because this mechanism is not included in GCMs modelled ice extents would be too small in winter around Antarctica, although simple models perform better in the Arctic because wind drift is less important. To generate an acceptable ice extent for climate studies, flux correction is also applied to sea ice.

4. Orographic Effects

The mass of the East Antarctic continent is well represented in GCMs, even though the steep slopes at the edge of the plateau have to be handled carefully to avoid numerical instabilities. West Antarctica is fairly well handled, but the Antarctic Peninsula is too small in the east-west direction, and too steep, to be correctly represented (Figure 1).

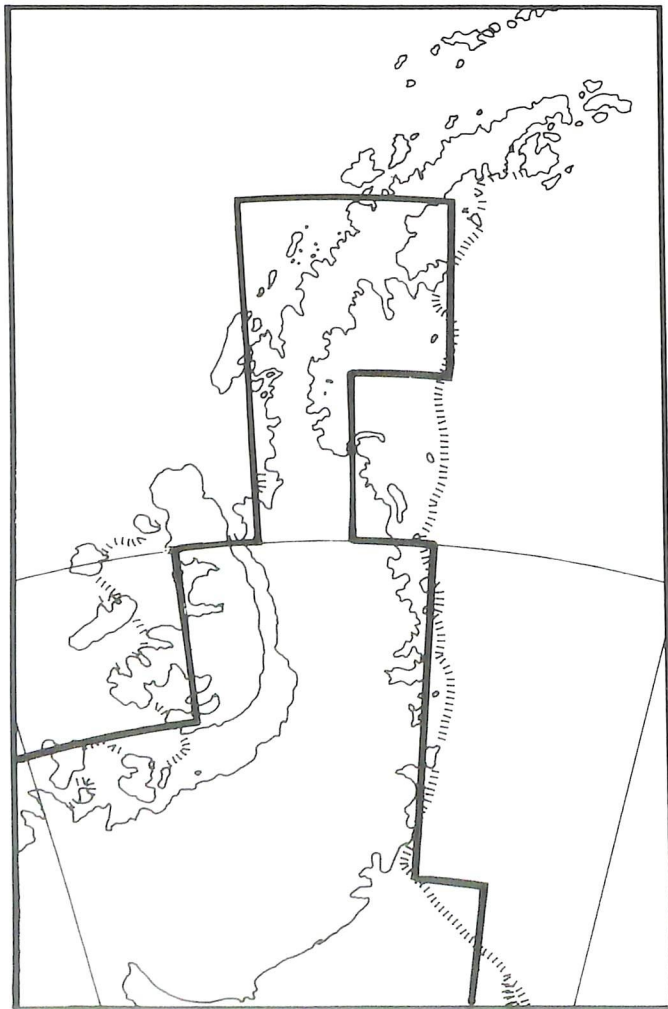


Figure 1. The coastline of the Antarctic Peninsula and the boundary between land/sea points in the GCM.

In the UKMO model it appears as less than half its true height and is therefore much less of a barrier to the model atmosphere. It is not yet clear whether this has implications for the global simulation, but it will certainly affect the simulation of, e.g. snowfall, on the peninsula.

5. Conclusions

Because of the above-mentioned problems detailed GCM predictions are not available for the Antarctic Peninsula. To obtain predictions a local area model forced by GCM output could be run over the peninsula area, but this would require considerable effort to verify a control simulation before any climate change studies could be done. Note that early predictions that the highest temperature rises would occur in the polar areas in winter (IPCC 1990) are not born out by more recent studies. The early studies were 'equilibrium' experiments, in which the steady-state response to a doubling of CO_2 was studied using a full GCM but a shallow ocean; more recent studies have been 'transient' runs in which CO_2 is slowly increased and a full ocean is included. In these, the effects of downwelling of heat into the oceans acts to cool the oceans around Antarctica.

6. References

- Hibler, W.D. (1979). A dynamic-thermodynamic sea ice model. *Journal of Physical Oceanography*, **9**, p. 815-846.
- IPCC (1990). *Climate Change. The IPCC Scientific Assessment*, Cambridge University Press, Cambridge.
- King, J.C. (1991). Recent climate variability in the Antarctic Peninsula. In Preprints, Fifth Conference on Climate Variations, *American Meteorological Society*, Boston. p. 354-357,
- Mitchell, J.F.B., and C.A. Senior (1989). The antarctic winter; simulations with climatological and reduced sea-ice extents. *Quarterly Journal of the Royal Meteorological Society*, **115**, p. 225-246.
- Simmonds, I. (1990). Improvements in general circulation model performance in simulating Antarctic climate. *Antarctic Science*, **2**, No. 4, p. 287-300.

ESTIMATING ICE-SHEET RESPONSE TO CLIMATE CHANGE

Richard C A Hindmarsh
British Antarctic Survey
Natural Environment Research Council
High Cross, Madingley Road
Cambridge, CB3 0ET
United Kingdom

Abstract

Procedures for estimating the likely response of ice-sheets to short-term climate change are given. These give estimates of the magnitude and rate of response, and the sensitivity of changes in divide thickness to changes in climate in the flanking areas.

1. Introduction

Changes in surface accumulation and temperature of an equilibrium ice-sheet will cause the equilibrium profile to change. It is now routine to compute such changes by numerical modelling. However, such a procedure is often rather involved, and involves a disproportionate amount of effort in those cases where the surface boundary conditions are not better than order of magnitude estimates. This article brings together some fairly well-known results for estimating the magnitude and the time-scale of response.

These results are for Antarctic type ice-sheets with fixed grounding lines.

2. Analytical solutions for steady profiles

The basic results we shall discuss were established by Vialov (1958), who considered the case of spatially uniform accumulation, a flat bed, and a margin with prescribed position with zero thickness. This model was extended by Nye (1959), who considered the influence of sliding and of axisymmetric geometries. I believe these simple models contain the essential physics of those Antarctic ice-sheets not drained by ice-streams. To demonstrate this, variations upon Vialov's model will be presented and shown not to make very much difference to the "physics".

It is a straightforward matter to alter Vialov's model to include a margin of prescribed thickness. However, it is not straightforward to solve analytically the differential equations when one wishes to include sloping beds and spatially varying accumulation. Instead, it is more convenient to divide the flow-lines

into longitudinal sections, each with a corresponding accumulation rate, rate-factor, constant bedrock elevation and flow-line width. The last is introduced in order to represent the Peninsula Ice Sheet, where the ice sheet along the ridge is drained by outlet glaciers.

This sectioned approach, where there are jumps in the properties, in particular in the bedrock elevation and the flow-line thickness, will produce several *local* violations of the approximation conditions for the governing equations. However, I believe the local response of the ice-sheet is passive; in other words, the flow of the ice at not very large distances from these zones of violation will "see" smoothed versions of these flows which respect the approximate equations.

Consider a co-ordinate system (x,z) with z vertical. The discharge $q(x)$ along a flow line is given by

$$q(x) = -\omega B (s - b)^{n+2} |s_x|^{n-1} s_x \quad (1)$$

where ω is the valley width divided by the valley spacing (no valleys implies $\omega = 1$), $z = s(x)$ is the surface elevation of the ice-sheet, $z = b(x)$ is the elevation of the base of the ice-sheet, x is the longitudinal position, subscript x indicates differentiation with respect to x and n is the index in Glen's law relating the stress τ and strain-rate d tensors:

$$d = A\tau^n \quad (2)$$

where A is the rate-factor, which is dependent upon temperature and other properties of the ice, like its moisture content and fabric. The rate factor A is usually supposed to have an Arrhenius-type dependence upon the absolute temperature T , i.e.

$$A = A_0 \exp\left(-\frac{E}{RT}\right), \quad (3)$$

where R is the gas constant and E is an activation energy for creep, though see Paterson (1981, p. 39).

The coefficient B in the flux formula is given by

$$B = \frac{2\bar{A}H_*^{2n+2}(\rho g)^n}{(n+2)a_*L_*^{n+1}} \quad (4)$$

where the subscript $*$ represents a scale magnitude, H is the divide thickness, L is the span, and a is the accumulation rate. This implies working in dimensionless units scaled by the appropriate scale magnitudes; those who do not like this procedure may take all the scale magnitudes as unity and end up with a definition of B as

$$B = \frac{2\bar{A}(\rho g)^n}{(n+2)}. \quad (5)$$

The quantity \bar{A} is a vertical average of A , given by

$$\bar{A}H = (n+2) \int_b^s \left(\frac{s-z}{H}\right)^{n+1} A dz \quad (6)$$

For steady-state, we require

$$\frac{dq}{dx} = a(x) \quad (7)$$

where $a(x)$ is the surface accumulation. Notice that by formulating thus, we are assuming that all the snow falling on ridges between outlet glaciers finds its way onto these outlet glaciers, either by avalanching or as ice in smaller, tributary glaciers.

We take the divide to be at $x = 0$, where the input discharge is zero. The downstream boundary condition is that the ice is of a specified thickness at $x = L_m$, the grounding line. We shall consider the cases of one, two and several sections, each with accumulation a_i , rate-factor A_i , width ω_i and bedrock elevation b_i , with $i = 1, 2, 3$. The position of the end of the section i is given by $x = L_i$. Thus, by construction, L_0 is the divide position and equals zero. We shall also wish to use an apparent section starting position \hat{L}_i given by

$$\hat{L}_{i-1} = \frac{\sum_{j=1}^{i-1} a_j L_j}{a_i} \quad (8)$$

and define the difference between the apparent and real section positions through

$$\Delta_i = \hat{L}_i - L_i. \quad (9)$$

Uniform accumulation rates will lead to $\Delta_i = 0$. We shall also on occasion work in a normalised horizontal co-ordinate $\xi = x/L_m$.

Combining relationships (7,1) and integrating twice yields

$$s(x) = b_i + \left(k_i - 2\alpha_i \frac{1}{n} (x - \Delta_{i-1})^{\frac{n+1}{n}}\right)^{\frac{n}{2n+2}} \quad (10)$$

where

$$\alpha_i = \frac{a_i}{\omega_i B_i} \quad (11)$$

and $q_i = \hat{L}_{i-1} a_i$ is the input discharge into section i .

We now consider one, two and several sections in turn. Clearly, section junctions must have matching elevations and discharges. The first condition will not hold exactly owing to reduced model violations, but we expect any apparent jump in thickness to be small.

2.1. One section models

One section models are the same as the Vialov model except that the margin thickness need not be zero. We have by construction $L_1 = L_m$, where $H_m = s_m - b_m$ is specified in terms of a flotation condition: if we have sea level at $z = 0$, we find $H_m = -\rho_{\text{water}} b_m / \rho_{\text{ice}}$, where ρ is the density.

Inserting the boundary conditions into (10) and rearranging yields

$$H^{\frac{2n+2}{n}} = H_d^{\frac{2n+2}{n}} \left(1 - \xi^{\frac{n+1}{n}}\right) + H_m^{\frac{2n+2}{n}} \xi^{\frac{n+1}{n}} \quad (12)$$

and

$$H_d^{\frac{2n+2}{n}} = H_m^{\frac{2n+2}{n}} + 2\alpha_1 \frac{1}{n} L_m^{\frac{n+1}{n}} \quad (13)$$

For $H_d \gg H_m$ we retrieve the Vialov solution and, through the definition of α in equation (11), the well-known result

$$H_d = 2^{\frac{n}{2n+2}} \left(\frac{a_1}{A_1}\right)^{\frac{1}{2n+2}} L_m^{\frac{1}{2}} \quad (14)$$

where we have taken $\omega = 1$. This, for $n = 3$, gives H_d as being proportional to the eighth root of the accumulation rate and the inverse rate factor. Thus, a doubling in the accumulation rate will yield a $2^{1/8} \approx 1.09$

increase in the ice sheet thickness. In fact, these results are so basic they can be obtained from the scalings; by considering (4), and noting that by construction of the scaling $B \sim 1$, then with all the other scales prescribed, we can solve for the thickness scale, and obtain this eighth-root result. These ideas have been used by Oerlemans (1991) to estimate the response of the Greenland ice-sheet to climatic change.

A more accurate statement of the inequality used to obtain (14) is

$$H_d^{\frac{2n+2}{n}} \gg H_m^{\frac{2n+2}{n}}$$

For $n = 3$ the power is $8/3$. If we want the left hand side of the inequality to be ten times the right hand side, this requires $H_d \approx 2.37H_m$.

In the more general cases where

$$H_d^{\frac{2n+2}{n}} \gg H_m^{\frac{2n+2}{n}}$$

we can obtain a similar result by differentiating H_d with respect to, for example, the accumulation rate. Thus,

$$\frac{dH_d}{da} = \frac{H_d}{a(2n+2)} \left[1 - \left(\frac{H_m}{H_d} \right)^{\frac{2n+2}{n}} \right] \quad (15)$$

If we are working in a scaled system ($H_d, a \sim 1$) it is immediately obvious that this is weak dependence, with similar numerical results to those obtained above for the case of H_m small. Notice that the greater the margin thickness, the *less* sensitive is the divide thickness to changes in the accumulation rate.

2.2. Two section models

By applying the margin thickness condition, we can solve for k_2 in equation (10). This may then be used to solve for the elevation s_{12} at the section junction, which is used to solve for H_d . We obtain

$$s_{12} = b_2 + \left[H_m^{\frac{2n+2}{n}} + 2\alpha_2^{\frac{1}{n}} \left((L_m + \Delta_1)^{\frac{n+1}{n}} - (L_1 + \Delta_1)^{\frac{n+1}{n}} \right) \right]^{\frac{n}{2n+2}} \quad (16)$$

and with the divide thickness given by

$$H_d^{\frac{2n+2}{n}} = (s_{12} - b_1)^{\frac{2n+2}{n}} + 2\alpha_1^{\frac{1}{n}} L_1^{\frac{n+1}{n}} \quad (17)$$

The profiles are given by typical hyper-elliptic

interpolates.

Let us write $H_{12}^- = s_{12} - b_1$, $H_{12}^+ = s_{12} - b_2$. Comparison of (17) with (13) shows that the thickness at the end of Section 1, H_{12}^- , has an identical functional role to the prescribed margin thickness in the one-section case, as one would expect. One expects similar sensitivity properties of the divide thickness to the accumulation rate. Partial differentiation of H_d in (17) with respect to a_1 and H_{12}^- , and then chaining the latter partial derivative with the derivative of H_{12}^+ with respect to a_2 , obtained from (16) yields

$$dH_d = \frac{H_d}{a_1(2n+2)} \left[1 - \left(\frac{H_{12}^-}{H_d} \right)^{\frac{2n+2}{n}} \right] da_1 + \left(\frac{H_{12}^-}{H_d} \right)^{\frac{n+2}{n}} \frac{H_{12}^+}{a_2(2n+2)} \left[1 - \left(\frac{H_m}{H_{12}^+} \right)^{\frac{2n+2}{n}} \right] da_2 \quad (18)$$

It is clear that the term which controls the relative sensitivity of a_2 with respect to a_1 is

$$\left(\frac{H_{12}^-}{H_d} \right)^{\frac{n+2}{n}} = \frac{\partial H_d}{\partial H_{12}^-} \quad (19)$$

Where the bed slopes down from the ice divide, $H_{12}^- < H_{12}^+$, and we expect the ratio H_{12}^-/H_d to be smaller than for the case of a flat bed. This will *reduce* the sensitivity of the divide thickness to changes in the accumulation rate of the flanking areas.

2.3. Several section models

More generally, we can write a recursion relationship;

$$s_{i-1,i} = b_i + \left[(s_{i,i+1} - b_i)^{\frac{2n+2}{n}} + 2\alpha_i^{\frac{1}{n}} \left((L_i + \Delta_{i-1})^{\frac{n+1}{n}} - (L_{i-1} + \Delta_{i-1})^{\frac{n+1}{n}} \right) \right]^{\frac{n}{2n+2}} \quad (20)$$

where $s_{i,i+1}$ is the elevation at the junction between section $i-1$ and section i . This may be rewritten

$$\left(H_{i-1,i}^+ \right)^{\frac{2n+2}{n}} - \left(H_{i,i+1}^- \right)^{\frac{2n+2}{n}} = 2\alpha_i^{\frac{1}{n}} \left((L_i + \Delta_{i-1})^{\frac{n+1}{n}} - (L_{i-1} + \Delta_{i-1})^{\frac{n+1}{n}} \right) \quad (21)$$

where the superscripts $-$, $+$ represent the thicknesses immediately upstream and downstream of a section junction.

Because the thicknesses are raised to the power $(2n+2)/n$, this formula shows that (as expected) the

influence of the "local" term (the right hand side) is exaggerated. This is especially true where the bedrock slopes down away from the divide, as $H_{i,i+1}^- < H_{i,i+1}^+$.

To analyse sensitivity a little more carefully, let us differentiate the section inlet thickness $H_{i-1,i}^+$ given by (21) with respect to the accumulation and with respect to the section outlet thickness $H_{i,i+1}^+$. We obtain

$$\frac{\partial H_{i-1,i}^+}{\partial a_i} = \frac{H_{i-1,i}^+}{a_i(2n+2)} \left[1 - \left(\frac{H_{i,i+1}^-}{H_{i-1,i}^+} \right)^{\frac{2n+2}{n}} \right] \quad (22)$$

and

$$\frac{\partial H_{i-1,i}^+}{\partial H_{i,i+1}^-} = \left(\frac{H_{i,i+1}^-}{H_{i-1,i}^+} \right)^{\frac{n+2}{n}} \quad (23)$$

If we take $H_{i-1,i}^+ = 1$, $a = 1$ this implies $H_{i,i+1}^-/H_{i-1,i}^+ < 0.29$ in order for the section inlet change to be more sensitive to an accumulation change than to a change in the outlet thickness.

As in the two-section model, we can investigate the sensitivity of the divide thickness to the section accumulation rates by chain differentiation. We find

$$dH_d = \frac{H_d}{(2n+2)} \left[1 - \left(\frac{H_{12}^-}{H_d} \right)^{\frac{2n+2}{n}} \right] \frac{da_1}{a_1} +$$

$$\left(\frac{H_{12}^-}{H_d} \right)^{\frac{n+2}{n}} \left(\frac{H_{12}^+}{(2n+2)} \left[1 - \left(\frac{H_{23}^-}{H_{12}^+} \right)^{\frac{2n+2}{n}} \right] \frac{da_2}{a_2} + \dots + \right. \quad (24)$$

$$\left. \left(\frac{H_{i,i+1}^-}{H_{i-1,i}^+} \right)^{\frac{n+2}{n}} \left(\frac{H_{i,i+1}^+}{(2n+2)} \left[1 - \left(\frac{H_{i+1,i+2}^-}{H_{i,i+1}^+} \right)^{\frac{2n+2}{n}} \right] \frac{da_{i+1}}{a_{i+1}} + \dots \right) \right.$$

The downstream changes in accumulation are successively multiplied by

$$\left(\frac{H_{i,i+1}^-}{H_{i-1,i}^+} \right)^{\frac{n+2}{n}}$$

that is, there is a declining geometric progression of

sensitivity. As before, the rate of decline of sensitivity is enhanced by having the bed sloping down from the divide.

2.4. Valley width and rate factor

The valley width divided by the valley spacing ω appears in the coefficient $\alpha = a/\omega B$. All the analysis we have done with regard to the accumulation rate applies in exactly the same way to ω and B ; in other words, divide thickness is not terribly sensitive to these quantities. This has the further implication that we do not have to worry very much about side-wall friction, as it enters into the flux formula (1) in the same way as do B and ω . This is Nye's (1965) "shape" factor.

3. Dynamic effects

The arguments presented in the previous section suggest that changes in steady-state thickness will be quite small, and that the ratio of the steady-state thicknesses before and after perturbation will be the ratio of the accumulation magnitudes raised to the power of one eighth.

This presupposes smooth behaviour of the steady-state solution with the controlling parameters. Non-smooth variations have been found (e.g. Oerlemans, 1981; Payne and Sugden, 1990), but while these are associated with topographic effects, they are also associated with ablating margins. There has never been any suggestion that these modified Vialov-Nye scenarios, *where the grounding line is prescribed*, have non-smooth variation of steady-state volumes.

Non-smooth variations associated with changes in the grounding zone position have been proposed (Weertman, 1974; Thomas and Bentley, 1978). While many glaciologists would agree that this is possible, it has not been demonstrated by any model which represents the mechanical details of the grounded ice-floating ice transition at all well. Moreover, while the non-smooth transitions occurring in the presence of ablation are fairly well understood in terms of associated steady and unsteady states (e.g. Oerlemans, 1981; Hindmarsh, 1990), no such understanding exists for ice-sheets discharging into ice-shelves.

Our best guess is that the glaciers discharging the Antarctic Peninsula and draining into the smaller fringing ice-shelves are less susceptible to putative grounding line instabilities than are the giant ice-streams disgorging into the Ross and Ronne-Filchner ice-shelves. This is related to the higher basal friction believed to be experienced by the Peninsula glaciers, which means they cannot "feel" changes in

downstream back-pressure; moreover, the passive ice-shelves into which they discharge are less likely to produce large changes in backpressure as are the enclosed Ross and Ronne-Filchner.

If we accept the arguments for small changes, then it is appropriate to conceptualise changes between these states as a linear perturbation. The system will relax exponentially onto the new state, with a time constant t_* given by

$$t_* = \frac{H_*}{a_*} \quad (25)$$

this is an order of magnitude estimate for the time scale of re-equilibrium (Nye, 1960; Johannesson et al., 1989; Hindmarsh, 1990). If we take $H_* = (500 \rightarrow 1000)\text{m}$, $a_* = (0.5 \rightarrow 1)\text{m/yr}$, we find $t_* = (500 \rightarrow 2000)$ years, significantly longer than the mooted time-scales of forcing for global change.

The accuracy of this estimate is only order of magnitude; thus we do not need to worry whether we use the accumulation rate before or after perturbation. Equally, the accuracy of this estimate is unlikely to be affected by whether the ice-sheet is currently in equilibrium, or indeed ever was. (This is *not* the same as saying that we can disregard disequilibrium in mass-balance calculations, which of course we cannot).

It is of interest to explore the dynamical response of an ice-sheet to a change in accumulation rate in a little more detail. Firstly, we scale time by the time constant t_* . We retain H_d as denoting the equilibrium thickness, but now for the *instantaneous* accumulation rate; thus, it makes sense to consider a quantity H_{dd} . Rearrangement of (14) (and dropping the sectional subscript) yields

$$a = \frac{H_d \left(\frac{2n+2}{n}\right)}{L_m \left(\frac{n+1}{n}\right)} \frac{A}{2^n} \quad (26)$$

which suggests we use the rhs as a viscous settling term. Thus, denoting H_{dd} as the dynamic divide thickness, we write down

$$\dot{H}_{dd} = a - \frac{H_{dd} \left(\frac{2n+2}{n}\right)}{L_m \left(\frac{n+1}{n}\right)} \frac{A}{2^n} \quad (27)$$

as a physically motivated approximation. We are in effect ignoring the dynamical effects of changes in the

normalised profile of the ice-sheet, but we expect solutions to this equation to capture the qualitative dynamics adequately.

Let us consider a perturbation in the thickness h , such that $H_{dd} = h + H_d$, where, we reiterate, H_d is the instantaneous equilibrium thickness. Assuming $h \ll H_d$, expanding H_{dd} and cancelling out the instantaneous accumulation rate with the term representing viscous settling due to the instantaneous equilibrium thickness yields

$$\dot{h} + \frac{nH_d}{(2n+2)a} \dot{a} = -\frac{a}{H_d} h \left(\frac{2n+2}{n}\right) \quad (28)$$

If we assume changes in H_d and a are small, and write the initial values of these quantities as H_{d0} , a_0 , and also write

$$\lambda = \frac{(2n+2)a_0}{nH_{d0}}$$

solution of (28) yields

$$h(t) = K \exp(-\lambda t) - \frac{\dot{a}}{\lambda^2} \quad (29)$$

where K is the constant of integration, which depends upon the initial conditions.

Firstly we consider a jump in the accumulation rate, which produces a new equilibrium thickness H_{d1} . After this jump, $\dot{a} = 0$. The solution to (29) is

$$\begin{aligned} h(t) &= (H_{d1} - H_{d0}) \exp(-\lambda t) \\ H_{dd} &= H_{d0} + (H_{d1} - H_{d0}) (1 - \exp(-\lambda t)) \end{aligned} \quad (30)$$

A better approximation for the Peninsula might be a period of constant accumulation, which has ended relatively recently, followed by a period of constantly increasing accumulation. Then, (29) yields

$$\begin{aligned} h(t) &= \frac{-\dot{a}}{\lambda^2} (1 - \exp(-\lambda t)) \\ H_{dd} &= H_{d0} + \frac{\dot{a}t}{\lambda} - \frac{\dot{a}}{\lambda^2} (1 - \exp(-\lambda t)) \end{aligned} \quad (31)$$

which implies that the difference h between the instantaneous thickness and the instantaneous equilibrium thickness settles to a value $-\dot{a}/\lambda^2$; if $\dot{a} > 0$, $h < 0$.

4. Thermal Effects

Apart from its direct effect upon surface mass

exchange, temperature also affects the flow of ice because the rate-factor A , and thus the coefficient B in (1) are dependent upon the temperature.

The scaling and the Vialov solution both give

$$H_d \propto B^{\frac{-1}{2n+2}}$$

More generally, the rate-factor always appears as a divisor of the accumulation rate in these steady solutions. This is obvious on dimensional grounds. Thus, all the comments about sensitivity of thickness to accumulation rate apply equally to the rate factor.

The problem is that while we might expect factor of two changes in the accumulation rate, it is quite reasonable, as we shall see, to expect factor of ten changes in the rate-factor. An *increase* in the rate-factor of this magnitude would reduce the thickness of the ice-sheet by one quarter ($10^{-1/8} \approx 0.75$).

Glacier temperature is affected by the climate-dependent upper surface temperature. The average rate factor \bar{A} given by (6) weights very heavily towards the rate-factor in the lowest part of the glacier. In order to estimate the response of ice-sheet geometry to surface temperature change, we must (i) know how long it takes for the basal layers to experience a surface temperature change, and (ii) estimate the magnitude of the change.

The bases of the flanking areas of an ice-sheet almost always reach melting point (e.g. Huybrechts and Oerlemans, 1988; Hindmarsh et al., 1989; Hindmarsh, 1990), so any change in surface temperature will not affect the basal temperature in these regions.

The basal temperature in the central regions is effectively determined by a linear vertical advection-diffusion equation. The time constant for surface changes to reach the base is the same as given in the previous section (Hanson and Dickinson, 1987; Hindmarsh, 1990), while the linear nature of the equation means that temperature solutions can be superposed; a ten degree change in the surface temperature will result eventually in a ten degree change in the basal temperature (in the absence of accumulation rate changes).

If we have an increase in the surface temperature, we would expect the upstream boundary of the zone of marginal zone of melting to move back (see Hindmarsh et al., 1989). How much we would expect it to move is not at all well understood, although we can expect to determine whether or not the base of the central region will be molten. By applying the chaining

results of the accumulation sensitivity study, we would not expect the divide thickness to be changed a great deal by changes in the rate-factor in the marginal area.

We are thus left with considering changes in the basal temperature in the central areas of an ice-sheet. While the temperature changes are superposable, rate-factors, being non-linear functions of temperature are not. A ten degree temperature change from -10°C to 0°C results in a ten-fold increase in rate-factor, while a temperature increase from -30°C to -20°C results in less than a three-fold increase in rate factor (ice-sheet thickness reduced by an eighth). Notice that the Arrhenius form of the dependence of rate-factor upon temperature (3) implies that a decrease in temperature from a given point has a smaller effect on rate-factor than an equivalent increase.

Basal temperature in the central area of a steady-state ice-sheet can be related to the surface temperature using the method developed by Robin (1955), and developed further by Clarke et al. (1977) and Paterson (1981).

Let T denote temperature, T_s the surface temperature and T_b the basal temperature. From the derivation in Paterson (1981, p.203) it is easy to show that where $Ha > 200\text{m}^2/\text{yr}$,

$$T_b - T_s \approx 0.2 \left(\frac{H}{a} \right)^{\frac{1}{2}} \quad (32)$$

where we are *not in a dimensionless system*; thicknesses are in metres, accumulation rates in metres per year, and temperatures in degrees Kelvin. The numerical terms in this equation are a function of the thermal properties of ice and the geothermal heat gradient. If we take $H = (500 \rightarrow 1000)\text{m}$, $a = (0.5 \rightarrow 1)\text{m}/\text{yr}$, we find $T_b - T_s = (5 \rightarrow 9)\text{K}$. With annual average surface temperatures ranging from -15°C to -20°C , this gives basal temperatures between approximately -5°C to -15°C .

Differentiation yields

$$dT_b = dT_s + \frac{T_b - T_s}{2} \left(\frac{dH}{H} - \frac{da}{a} \right) \quad (33)$$

We do not really expect changes in H to be large. Notice, however, that if an increase in temperature leads to an increase in the accumulation rate as expected, while on the one hand increased surface temperature will lead to an increased basal temperature, on the other hand increased vertical velocities will advect more cold downwards, and that in consequence the basal temperature could either increase or decrease.

However, it is possible that the basal areas of the central region could experience several degrees of warming, depending upon the degree of warming of the polar atmosphere, with a dangerous scenario being that basal temperatures were increased from say -10°C to melting point, and the steady-state thickness reduced by about a quarter. This would be delayed compared with any build-up due to increased accumulation by a time period of order t_c . If the base *did* warm, we would expect an initial build up of the ice due to increased accumulation, followed by a decay due to basal warming somewhat later. On the other hand, if increased accumulation rates lead to basal cooling, the increase in ice-sheet thickness would be greater, and sustained over a longer period.

5. Conclusions

(i) Scaling analyses suggest that thickness is proportional to the one eighth power of the accumulation rate. This result appears to hold for Peninsula type configurations. There is a similar weak dependence upon the temperature-dependent rate factors and the width of the outlet valleys.

(ii) Steady-state thickness changes in the Peninsula are most sensitive to changes in the accumulation rate in the central reservoir regions. The effect of the bedrock sloping down from the central areas reduces the influence of changes in the flanking areas. This result could be better defined by a numerical study.

(iii) In the absence of any convincing theoretical suggestions for the existence of multiple steady and unsteady states, we suppose that smooth changes in the governing parameters (in effect, accumulation rate) will produce smooth changes in ice-sheet volume.

(iv) Changes between steady-states may then be adequately described by an exponential relaxation model, with a time scale given by the thickness magnitude divided by the accumulation rate magnitude. This gives a time scale for re-equilibration of between five hundred and two thousand years.

(v) Surface temperature changes will propagate to the base according to this same timescale. The opposing effects of increased surface temperature and increased advection of cold could result in basal temperatures either increasing or decreasing, and ice-sheets experience either additional thickening or thinning as a result of surface temperature increase.

6. References

- Clarke, G K C, U Nitsan and W B Paterson (1981). Strain-heating and creep instability in glaciers and ice-sheets. *Review of Geophysics and Space Physics*, **15**, p. 235-247.
- Hanson, B and R E Dickinson (1987). A transient temperature solution for bore-hole model testing. *Journal of Glaciology*, **33**, p. 140-148.
- Hindmarsh, R C A (1990). Time-scales and degrees of freedom operating in the evolution of continental ice-sheets. *Transactions of the Royal Society Edinburgh*, **81**, p. 371-384.
- Hindmarsh, R C A, G S Boulton and K Hutter (1989). Modes of operation of thermo-mechanically coupled ice-sheets. *Annals of Glaciology*, **12**, p. 57-69.
- Huybrechts, P H and J Oerlemans (1988). Evolution of the East Antarctic ice-sheet: a numerical study. *Annals of Glaciology*, **11**, p. 52-59.
- Johannesson, T, C R Raymond and E D Waddington (1989). Time-scale for the adjustment of glaciers to mass-balance. *Journal of Glaciology*, **35**, p. 355-369.
- Nye, J F (1959). The motion of ice-sheets and glaciers. *Journal of Glaciology*, **3**, p. 355-369.
- Nye, J F (1960). The response of ice-sheets and glaciers to seasonal and climatic changes. *Proceedings of the Royal Society A*, **256**, p. 559-584.
- Nye, J F (1965). The flow of a glacier in a channel of rectangular, elliptic or parabolic cross-section. *Journal of Glaciology*, **5**, p. 661-690.
- Oerlemans, J (1981). Some basic experiments with a vertically-integrated ice-sheet model. *Tellus* **33**, p. 1-11.
- Oerlemans, J (1991). The mass-balance of the Greenland ice-sheet: sensitivity to climate change as revealed by energy-balance modelling. *The Holocene* **1**, p. 40-49.
- Paterson, W S B (1981). *The physics of glaciers* (2nd Edition), Oxford, Pergamon Press.
- Payne, A J and D E Sugden (1990). Topography and ice-sheet growth. *Earth Surfaces, Processes and Landforms* **15**, p. 625-639.
- Robin, G de Q (1955). Ice-sheet movement and temperature distribution in glaciers and ice-sheets. *Journal of Glaciology*, **2**, p. 523-532.

Thomas, R H and C R Bentley (1978). A model for the Holocene retreat of the West Antarctic ice-sheet. *Quaternary Research* **10**, p. 150-170.

Vialov, S S (1958). Regularities of ice deformation. IASH Symposium of Chamonix, Physics and movement of ice, IAHS publ. 47, p. 383-391.

Weertman, J (1974). Stability of the junction of an ice-sheet and an ice-shelf. *Journal of Glaciology*, **13**, p. 3-11.

THE ICE SHELVES OF THE ANTARCTIC PENINSULA: CHANGING CLIMATE AND SEA LEVEL

David G Vaughan
British Antarctic Survey
Natural Environment Research Council
High Cross, Madingley Road
Cambridge, CB3 0ET
United Kingdom

Abstract

The recent changes in extent of the ice shelves of the Antarctic Peninsula are reviewed and the implications for the sea level discussed in the light of the measured regional warming. Data is presented that imply the disintegration of Wordie Ice Shelf has not been accompanied by an immediate increase in velocity on the input glaciers. Despite the relatively large component of basal sliding, backpressure from the ice shelf does not appear to have been important in their force balance. Even the complete disintegration of the ice shelves on the Antarctic Peninsula is thus unlikely to cause a globally significant amount of grounded ice to melt or noticeable sea level rise.

The ice shelves of the Antarctic Peninsula may, however, have a strong influence on regional climate and are certainly robust indicators of climate change. They also provide an excellent training ground to study ice shelves on the move, in preparation for making reliable predictions about the fate of ice shelves further south that stabilize the West Antarctic Ice Sheet.

1. Introduction

Frolich (this report) estimates that the area of grounded ice in the Antarctic Peninsula is about 330 000 km² and that of its ice shelves is about 150 000 km². This high ratio of ice shelf area to grounded catchment area compared to the rest of Antarctica reflects the unusually high accumulation rate on the Antarctic Peninsula (Doake, 1984), as well as its highly sinuous coastline.

Morrison (1990) presented mean annual air temperature records for Faraday Base (1957-1989) and Marguerite Bay (1962-1989). A cool period throughout the 1960s and was followed by warm periods in the early 1970s and 1980s. Temperatures have risen since 1986, with 1989 being the warmest year on record in both areas. Simple linear regression of the Faraday mean annual air temperature record shows an increase of 0.064°C a⁻¹ since records began in 1957, a total of around 1.5°C. The statistical significance of this value for long term trends is open to question and has been discussed at length by Sansom (1989). What is, however, certain is that climate on the Antarctic Peninsula has shown a warming over the past 30 years.

Associated with this temperature rise are considerable

changes in the extent of ice shelves around the Antarctic Peninsula over the past 30 years. I shall discuss the reported recent changes and current state of mass balance of the ice shelves on the Antarctic Peninsula and the implications for sea level.

2. Effect of ice shelf changes on sea level

Ice shelves are by definition floating and displace their own mass of sea water. Consequently, any reduction in overall volume of ice shelves has no direct effect on sea level. There are, however, indirect processes that could cause changes in ice shelf extent or thickness to alter the volume of grounded ice and thus make a contribution to sea level change.

It has long been maintained that the major Antarctic ice shelves (i.e. Ronne/Filchner, Ross) play a significant role in restraining the West Antarctic Ice Sheet (Bindschadler, 1990; Hughes, 1973; Mercer, 1978; Thomas et al., 1979). The West Antarctic Ice Sheet (WAIS) is thought to be uniquely vulnerable since it is grounded on bedrock that is mostly below sea level.

The vast majority of the ice leaving the interior the WAIS is channelled through ice streams and the

controls on ice stream velocity are of crucial importance to the mass balance of the ice sheet. Ice shelves provide a major restraint on ice streams by exerting on them a "backpressure" (MacAyeal, 1987). Removal of the ice shelves, and consequent removal of the backpressure would cause thinning of the ice stream at the grounding line and hence an inland migration of the grounding line. Since the bedrock beneath is below sea level, an initially small retreat in the grounding-line might initiate a positive feedback and a rapid retreat might follow. It has been estimated that total collapse of WAIS would cause a rise in global sea level of around 5 m.

The Antarctic Peninsula ice cover and the East Antarctic Ice Sheet (EAIS) are considered more robust in this respect, primarily because the ice rests on bedrock that is mostly above sea level. On the Antarctic Peninsula there is a further consideration; glaciers are mostly constrained by bedrock topography to flow in the valleys. Rather than a single sheet it should be considered as a complex mountain glacier system, where individual glaciers have well defined patterns of accumulation and ablation, and catchment basins constrained by bedrock topography. The system is more dynamic and typical ice residence times much less than on either WAIS or EAIS. Prediction of the response of this type of glacier system to projected climate scenarios will be particularly complex and will require modelling on a higher spatial and temporal resolution than that needed for either WAIS or EAIS.

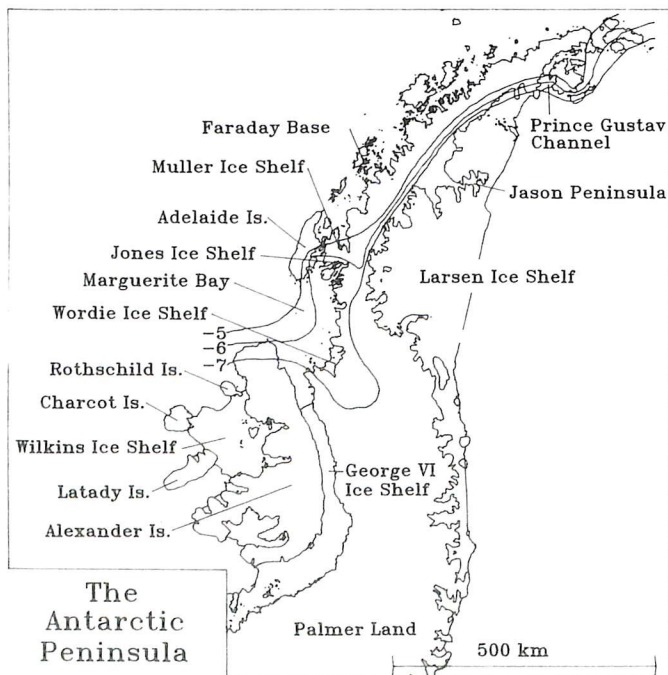


Figure 1. The location and distribution of ice shelves on the Antarctic Peninsula. Solid lines mark contours of 10 m temperature ($^{\circ}\text{C}$) normalised to sea level after Reynolds (1981).

3. Ice shelf distribution

There is apparent disparity in the latitudinal limit of ice shelves on the east and west coast of the Peninsula (Figure 1). Reynolds (1981) noted that the measured 10 m temperatures normalised to sea level were on average 7°C warmer in the central and western regions of the Peninsula, compared to locations on the east of the Peninsula at similar latitudes. The ridge of the Antarctic Peninsula thus marks the boundary between two very different climatic regimes.

The northerly limit for ice shelves on the west coast of the Antarctic Peninsula is marked by a group of ice shelves between Adelaide Island and the Antarctic Peninsula (e.g. Jones Ice Shelf and Muller Ice Shelf). These ice shelves are very small, having areas less than 50 km^2 , and so are not considered worthy of detailed discussion here, being very different in nature to the large ice shelves. They occur upstream of narrow constrictions and are said to survive only because of the sheltered fjord environment (Swithinbank, 1988).

The northern limit of ice shelves of significant area (over 100 km^2) on the west coast was until recently, Wordie Ice Shelf at 69° S . On the east coast the most northerly ice shelf is that section of Larsen ice shelf within Prince Gustav Channel, at 64° S .

Mercer (1978) noted that distribution of ice shelves might be climatically controlled, with the 0°C summer isotherm marking the limit of viability. He went on to speculate that a warming climate might induce the demise of some of the "marginal ice shelves", namely, the Prince Gustav Channel section of Larsen Ice Shelf, Wordie Ice Shelf, George VI Ice Shelf and Wilkins Ice Shelf.

Reynolds' (1981) compilation of 10 m temperatures shows that the -5°C mean annual temperature also successfully marks the ice shelf limit, although the -6.5°C isotherm probably more adequately marks the limit of ice shelves over 100 km^2 . This observation alone, however, provides no physical explanation of the processes controlling the limit of viability. A better approach is made by relating mass balance parameters (precipitation and ablation) to mean annual air temperature (Doake and Vaughan, 1991). This procedure has previously been used for climate modelling (Pollard, 1980; Oerlemans, 1982). For temperatures higher than -12°C the net accumulation (M) can be expressed as a function of the precipitation (P), the mean annual temperature (T) and a parameter (m) related to the ablation rate by

$$N = P - m(12 + T)^n$$

where $n = 1$ for Pollard's linear model or $n = 2$ for Oerlemans' quadratic model - and P has been assumed to be independent of T - for simplicity over the relatively small temperature range of interest here. There thus emerges a critical temperature, below which the net accumulation is positive (mass gain) and above which it is negative (mass loss); this is around -5°C . Over the Antarctic Peninsula, however, the dearth of measurements on which to base such parameterisations means that such treatments can at present only be considered as speculative. The operation of automatic weather stations will, perhaps, provide the best route for collecting adequate data to improve matters.

The marginal ice shelves of the Antarctic Peninsula thus provide a large scale indicator of changes in certain climatic parameters.

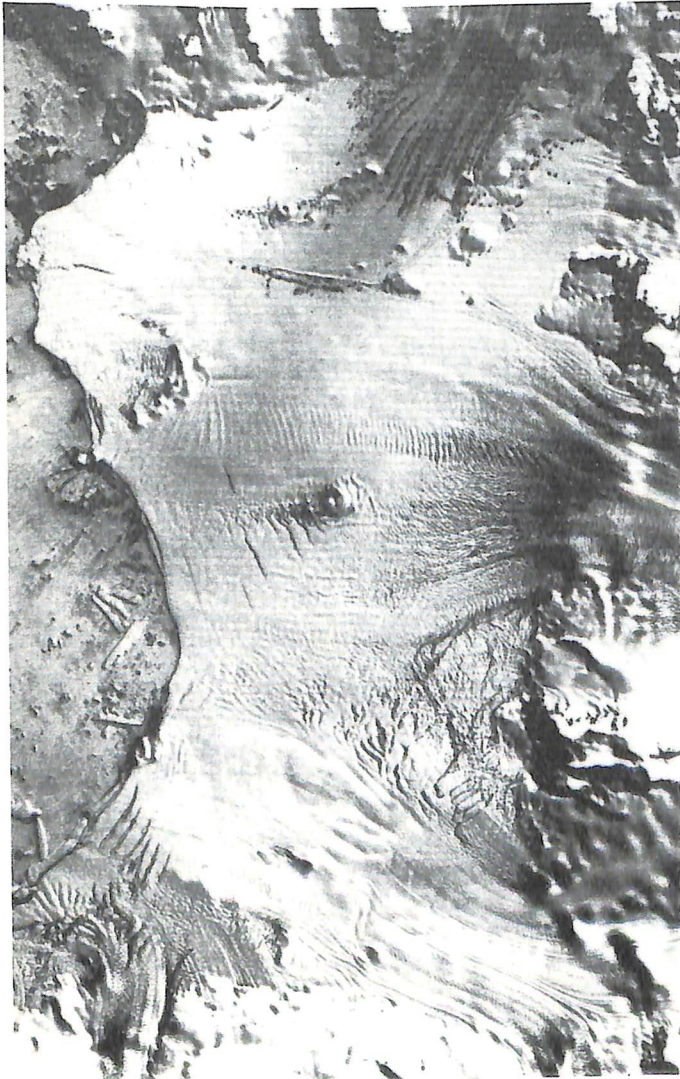


Figure 2(a). Landsat image showing the condition of Wordie Ice Shelf in 1974 (MSS).

4. Marginal ice shelves

4.1. Wordie Ice Shelf

Wordie Ice Shelf lies off the west coast of the Antarctic Peninsula. In the 1940s and 1950s it was regularly crossed by parties with dog teams but in the last few decades its extent has rapidly decreased to its present condition: little more than a few unconnected retreating glacier tongues.

4.1.1. Breakup of Wordie Ice Shelf

Doake and Vaughan (1991) have analysed Landsat images of the Wordie Ice Shelf taken in 1974, 1979 and 1989 (Figure 2) and images covering only the ice front portion taken in 1986 (Landsat) and 1988 (SPOT). The 1989 image was registered to surveyed ground control points and used as a base to which the other images were registered and resampled.



Figure 2(b). Landsat image showing the condition of Wordie Ice Shelf in 1979 (MSS).

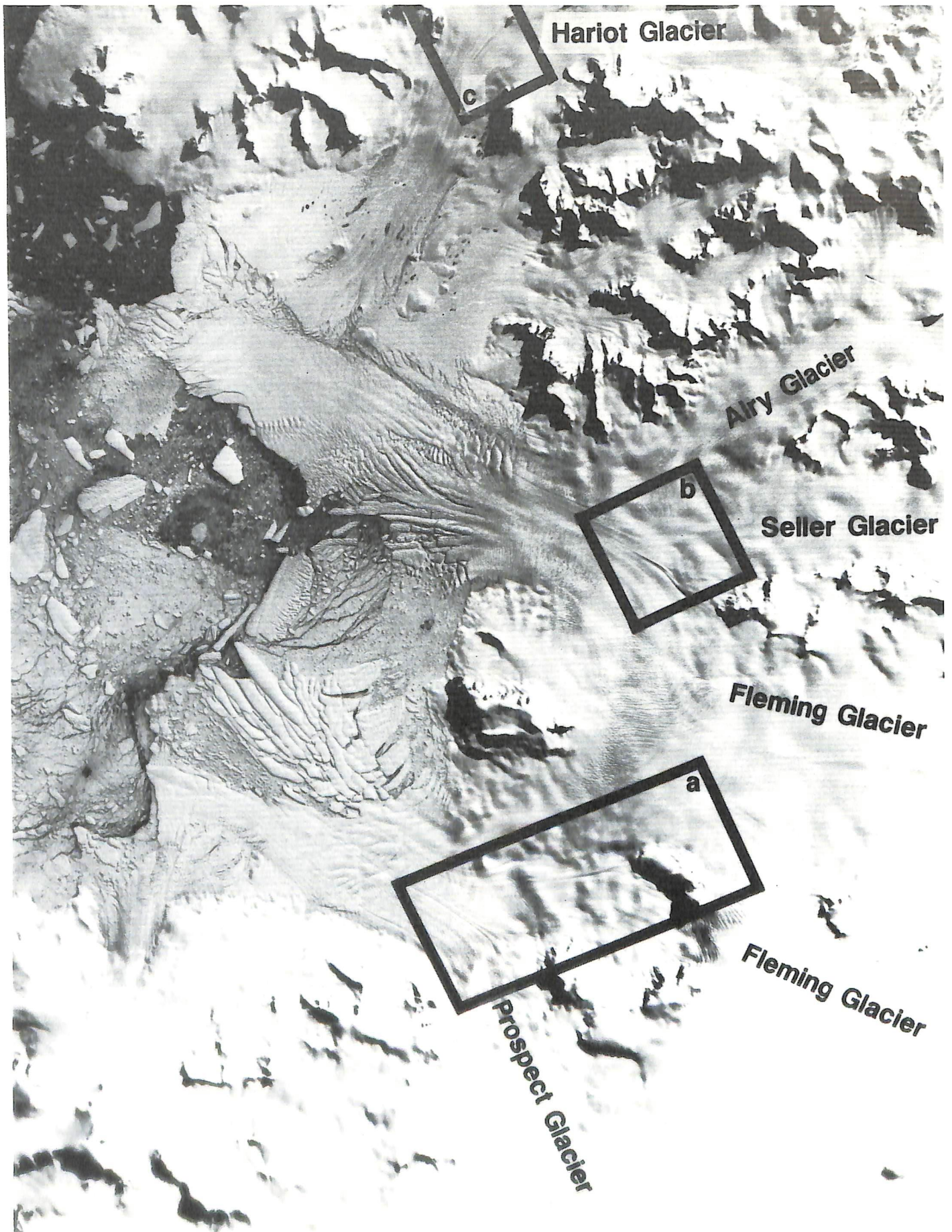


Figure 2(c). Landsat images showing the condition of Wordie Ice Shelf in 1989 (TM).
(All imagery is published courtesy of EOSAT).

Features in separate images were identified and matched to pixel size (25 m) and compared in position to an accuracy of about 50 m. Using the position of the ice front in 1966 mapped from aerial photography, they estimate that the ice shelf area has decreased from about 2000 km² in 1966 to about 700 km² in 1989. However, defining the position of the ice front can be very uncertain, with large blocks calving off to form icebergs being difficult to classify as being either attached to, or separated from, the ice shelf.

Analysis of the imagery and earlier maps shows that the ice front retreat has been punctuated by periods of stasis during which the ice front rests on ice rises. Retreat between periods of stasis is rapid. The major ice rises have thus played several roles in controlling the ice shelf behaviour. When embedded in the ice shelf, they created broken wakes downstream, and zones of compression upstream which helped to stabilise the ice shelf. During ice front retreat, they temporarily pinned the local ice front position and also acted as nucleating points for rifting which stretched upstream, suggesting that a critical fracture criterion had been exceeded. At this stage, an ice rise, instead of protecting the ice shelf against decay, aided its destruction by acting as an indenting wedge. Fracture of ice is a critical process in ice shelf dynamics (Hughes, 1983) and before we can understand ice shelf retreat mathematical models hitherto based on continuum mechanics (MacAyeal and Thomas, 1982; Lange and MacAyeal, 1989) will have to incorporate fracture mechanics to describe iceberg calving and how ice rises can initiate fracture both upstream and downstream.

Doake and Vaughan conclude that breakup was triggered by a climatic warming which increased ablation and the amount of melt water. Laboratory experiments show that the fracture toughness of ice is reduced at higher temperatures and possibly by the presence of water (Liu and Miller, 1979; Sabol and Schulson, 1989). Instead of refreezing in the upper layers of firn, free water could percolate down into crevasses and, by increasing the pressure at the bottom, allow them to grow into rifts (Robin, 1974) or possibly to join up with basal crevasses (Jezek, 1984). Processes like these would increase the production rate of blocks above that required for a "steady state" ice front position. The blocks will drift away as icebergs if conditions, such as bay geometry and lack of sea ice, are favourable. Thus, ice front retreat is, *inter alia*, a sensitive function of mean annual air temperature.

4.1.2. Effects on the grounded ice sheet

Changes in the flow of the grounded ice sheet could both drive and be driven by changes in the ice shelf.

The surge of an inland glacier can cause increased flux across the grounding line the ice shelf and hence changes in the ice shelf extent. Conversely, the ice shelf backpressure may limit the flow of inland glaciers.

In order to fully determine the effects of the disintegration of Wordie Ice Shelf on the inland ice sheet we should search for signs of both types of interaction. Fortunately, one type of observation appears to answer both questions.

Wordie Ice Shelf is fed by a number of tributary glaciers, which join to make three main input units (Figure 2). In the north, Meridian Glacier and Hariot Glacier merge at Confluence Cone, 12 km upstream of the grounding-line, then enter Wordie Ice Shelf as a single unit. The Airy, Seller and a portion of Fleming glaciers merge across the Forster Ice Piedmont, around 15 km upstream of the grounding-line, and the other portion of Fleming Glacier and Prospect Glacier merge close to the grounding-line in the south. Ridge-trough features are generated at the confluence of these glacier pairs; I call these "medial plumes" after MacAyeal's (1988) description of "relic crevasse plumes". These features are visible on the Landsat imagery and, in that they continue to delineate the glaciers for some distance downstream, resemble medial moraines.

It is reasonable to assume that each of the tributary glaciers has a different pattern and amount of sliding at its base, and hence a different balance between longitudinal and vertical shear stress. A change in the velocity of the glacier below the confluence, either due to a change in ice shelf backpressure or due a surging tributary would almost certainly cause a change in dominance of the tributaries. This would be manifest by a changed position of the median flowline. Figure 3 shows the sub-scenes of 1974 and 1989 Landsat images; the location of the sub-scenes are marked in Figure 2. Between 1974 and 1989 we can see no alteration in the positions of the medial plumes between Fleming Glacier and Prospect Glacier, between Seller Glacier and Fleming Glacier and between Median Glacier and Hariot Glacier. When accurately registered the medial plumes appear constant in position to at least the resolution of the images (70 m). We thus conclude that there has been no significant alteration in the flow of the inland ice, either, causing or responding to changes in the ice shelf extent.

In order for ice shelf backpressure to be significant in restraining a glacier, longitudinal stresses must be important in its force balance. This is certainly the case in a glacier sliding over its base. Muszynski and Birchfield (1987) showed that for sliding glaciers there is a direct mechanism linking ice shelf backpressure to

the strain rate of ice streams that feed it. Walford (1972) and Doake (1975) determined that the surface velocity of Fleming Glacier about 45 km upstream of the grounding line was around 0.5 m /day. Using a radio-echo fading pattern technique, they determined that up to 30% of the surface velocity is due to basal sliding. Presumably there is an increase in the relative amount of sliding towards the grounding-line.

4.2. Wilkins Ice Shelf

Wilkins Ice Shelf, has an area of 16 200 km² and lies off the west coast of the Antarctic Peninsula bounded by Alexander, Latady, Charcot and Rothschild islands. With the disintegration of nearby Wordie Ice Shelf we may well ask: how long will Wilkins Ice Shelf survive?

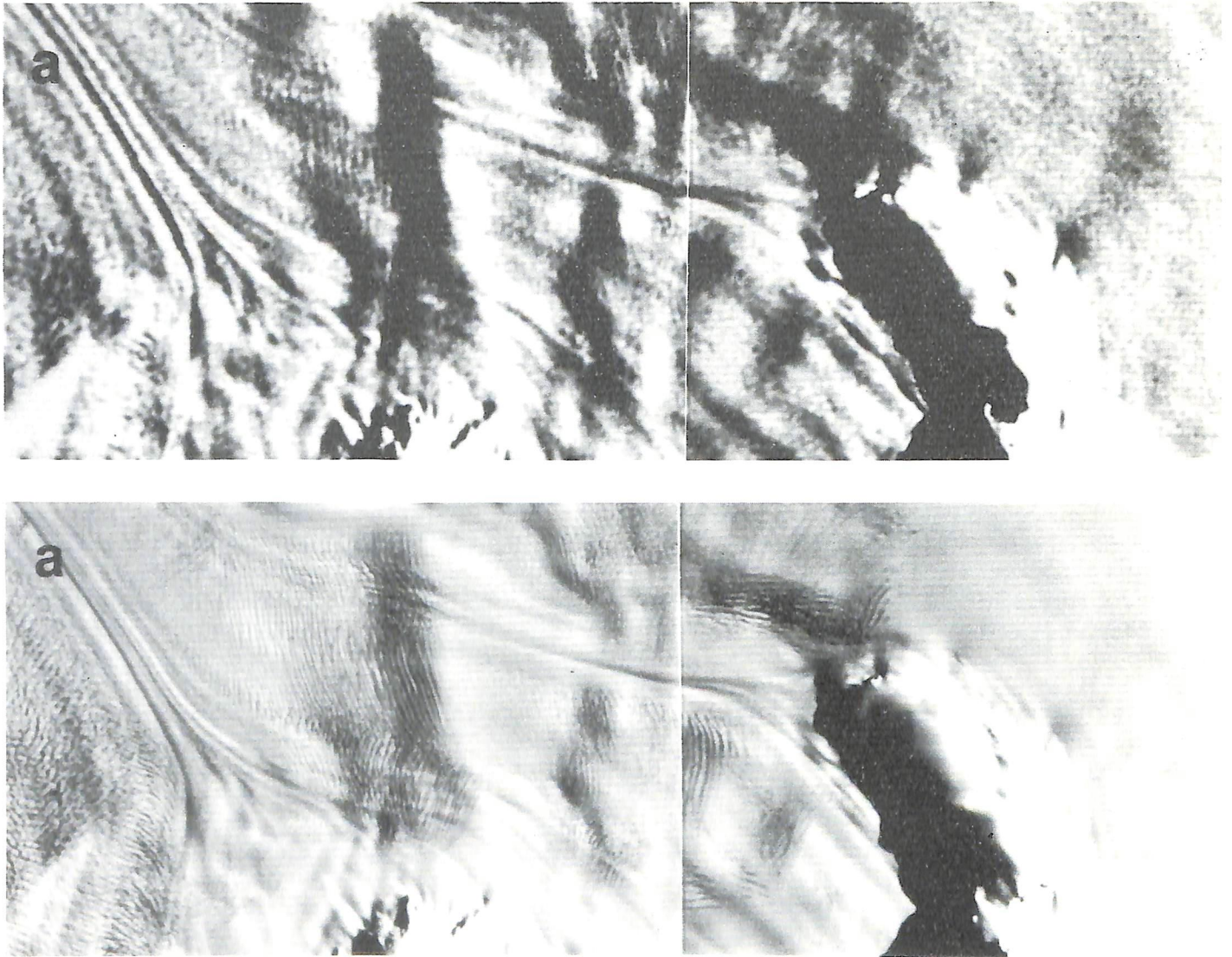


Figure 3(a). Landsat subsenceses showing medial plumes in 1974 (top) and 1989 (bottom) for Fleming and Prospect Glacier (20 x 8 km).

If the retreat of Wordie Ice shelf caused a significant change in backpressure at the grounding-line we should expect this to be transmitted upstream for some distance. At the points of confluence there has, however, been no change in the relative dominance of the tributary glaciers and we conclude that the ice shelf provided no significant restraint on the inland glaciers. Likewise the absence of fluctuation in the medial plumes shows flow in the tributary system to be stable, providing evidence that the disintegration of the ice shelf was not initiated by a glacier surge.

Compared to some other ice shelves on the Antarctic Peninsula few surface glaciological data have been collected on Wilkins Ice Shelf. Vaughan et al. (in press) have used a variety of remotely sensed data: the recently declassified GEOSAT Geodetic Mission altimetry, Landsat MSS and TM imagery, and radio-echo sounding data (RES), to study the structure and mass balance regime of Wilkins Ice Shelf.

The study highlights the strength of multi-sensor studies in aiding interpretation. GEOSAT Geodetic

Mission data yielded an excellent surface elevation/thickness map showing much structure. Contrast stretched Landsat TM imagery has proved to be a significant improvement on the earlier Landsat MSS photographic product, and has revealed many small ice rises and flowlines. The distribution of successful RES has shown the extent of the glacier ice and in situ accumulation. We now have a good structural model of Wilkins Ice Shelf which form a baseline for studies of change.

Vaughan et al. (in press) have however shown that Wilkins Ice Shelf is unusual for an Antarctic ice shelf in that it derives most of its sustenance from in situ accumulation and has low horizontal velocities. Its response to climate change may thus be very different to ice shelves fed by dynamic outlet glaciers. For instance, Wordie Ice Shelf began disintegrating by calving along its ice front while enhanced fracture processes were weakening its interior.

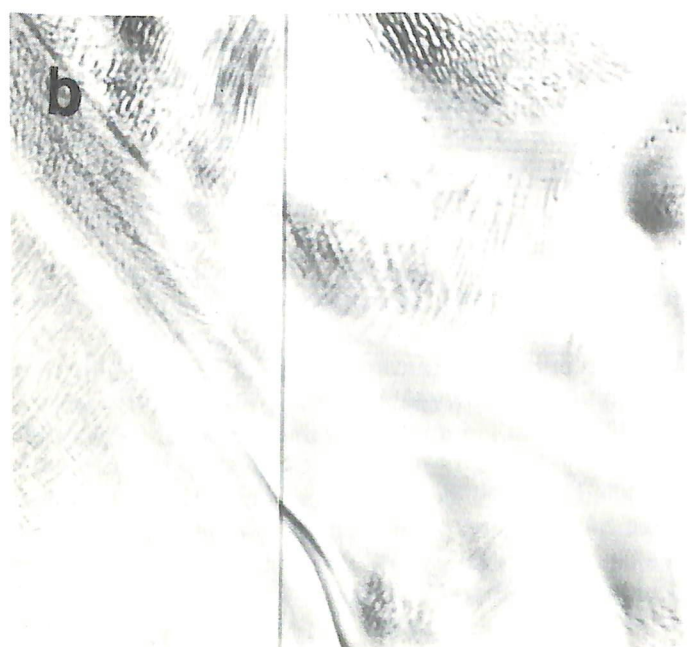
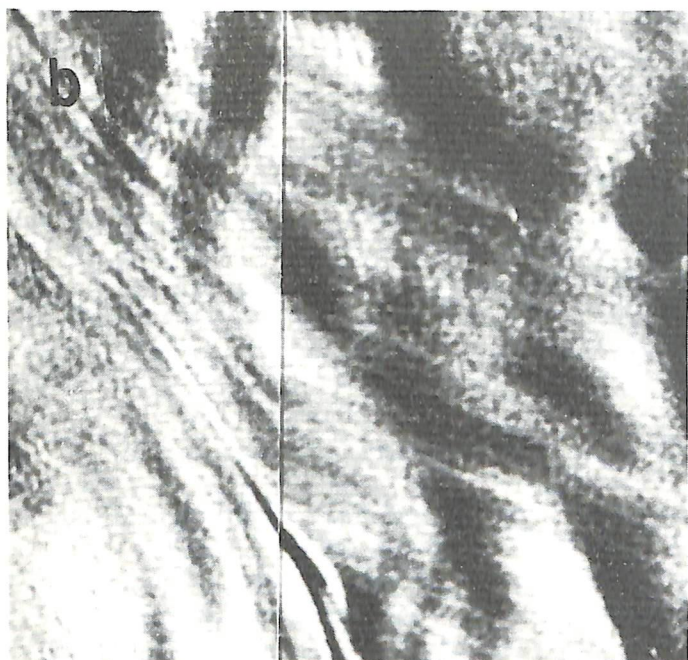


Figure 3(b). Landsat subscenes showing medial plumes in 1974 (top) and 1989 (bottom) for Seller and Fleming Glacier (9 x 9 km).

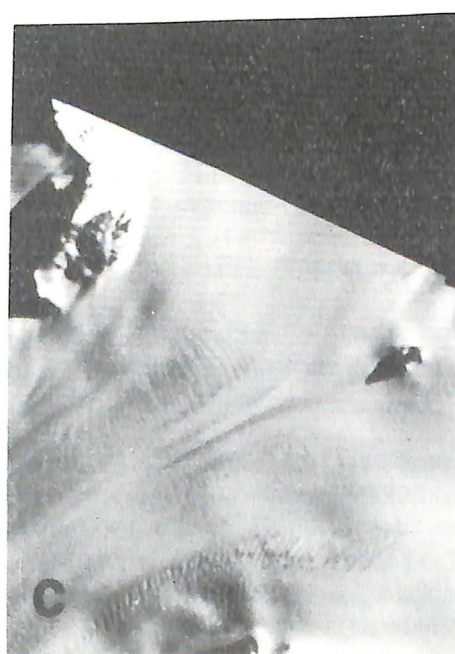


Figure 3(c). Landsat subscenes showing medial plumes in 1974 (top) and 1989 (bottom) for Median and Harriot Glacier (6 x 9 km).

After the ice front had decayed past a critical limit defined by pinning on ice rises and rumples, the outlet glaciers were able to punch through the remaining ice shelf because of the reduced restraint on them. The lack of such fast flowing glaciers entering Wilkins Ice Shelf means that a component important in the disintegration of Wordie Ice Shelf is absent. The ice front of Wilkins Ice Shelf is likely to decay by normal calving processes, which at present are still largely unknown, but there is unlikely to be the sudden disintegration seen on the Wordie, at least until the calving front decouples from the fringing islands. Over the last two decades the ice front positions have remained stable.

4.3. George VI Ice Shelf

Although some of the earliest records are difficult to interpret precisely, we may be confident that the northern ice front of George VI Sound was largely stable between 1949 and 1974, but by 1979 had retreated by around 15-20 km (Doake, 1982). We have observed from Landsat imagery that between 1979 and 1989 there have been further small retreats, amounting to a few kilometres.

Potter et al. (1984) have shown that the mass balance of George VI Ice Shelf is primarily a balance between glacier input ($45 \text{ km}^3 \text{ a}^{-1}$), *in situ* accumulation ($12 \text{ km}^3 \text{ a}^{-1}$) and basal melting ($53 \text{ km}^3 \text{ a}^{-1}$), iceberg calving being relatively insignificant ($4 \text{ km}^3 \text{ a}^{-1}$).

The response of George VI Ice shelf to a changing climate may thus be more sensitive to changes in ocean temperature and circulation or to changes in accumulation.

Since the glaciers that feed George VI Ice Shelf are steep and active mountain glaciers, even the complete removal of the ice shelf is unlikely to result in the loss of much grounded ice. The effect of its removal on sea level would be almost negligible.

4.4. Larsen Ice Shelf

Larsen Ice Shelf is more usefully considered in separate sections according to its distinct glaciological units.

During the 1940s Larsen Ice Shelf was reported to stretch unbroken between James Ross Island and Robertson Island (Figure 4). By 1957 there was a retreat of 15 km. Another 15 km retreat by 1969 separated the Prince Gustav Channel section from the section between Cape Longing and Robertson Island.

The Prince Gustav Channel section of Larsen Ice Shelf, originally identified by Mercer as being prone to

climate change, has been reported by various BAS personnel as continuing to deteriorate.

Skvarca (in press) has shown that the section between Robertson Island and Cape Longing was stable between 1969 and 1975 when the ice front showed little movement. Around 550 km^2 of the ice shelf were lost between 1975 and 1986. The retreat then accelerated and a further 550 km^2 were lost by 1989.

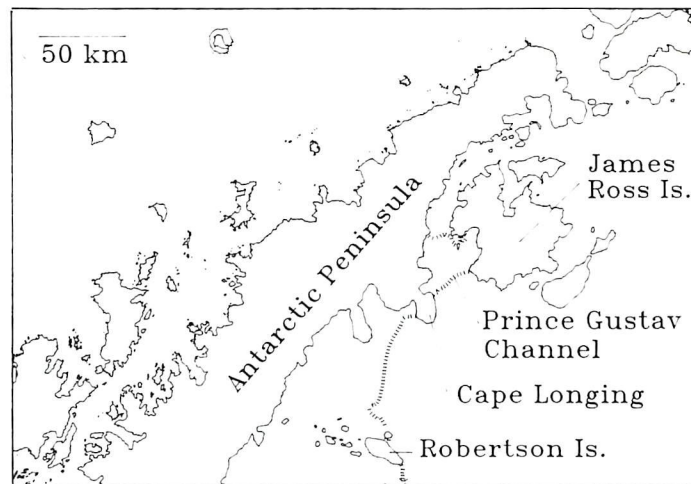


Figure 4. The northern section of Larsen Ice Shelf.

The longest temperature record in the region from the Orcadas station, South Orkney Islands, shows a 0.028°C per year average increase in mean annual temperature since records began in 1930.

The section of Larsen Ice Shelf south of Jason Peninsula has a 10 m temperature of below -11°C (Reynolds, 1981) so is not considered marginal. We note, however, that this portion of Larsen Ice Shelf has a very small grounded catchment area and so must be sustained (like Wilkins Ice Shelf) primarily by *in situ* accumulation. It may thus be very sensitive to changes in accumulation rate.

5. Discussion

Mercer's original statement that "one warning sign that a dangerous warming is beginning in Antarctica will be the breakup of ice shelves in the Antarctic Peninsula" is already being borne out. Of the ice shelves he identified as most likely to be affected, all but Wilkins Ice Shelf have shown continued retreat. For Wordie Ice Shelf and the northern section of Larsen Ice Shelf the changes are most dramatic.

We have, however, seen no noticeable contribution to sea level rise in response to the loss; and nor are we likely to in the future. The results presented here show

that even the complete removal of Wordie Ice Shelf has resulted in no appreciable velocity changes a few kilometres upstream of the grounding line. The theory of backpressure may indeed be valid to the large ice streams of WAIS but cannot be translated to the steep valley glaciers of the Antarctic Peninsula, even where significant glacier sliding is known to be occurring. If we can apply this result to the whole Antarctic Peninsula then even the complete removal of the marginal ice shelves over, perhaps, the next 50 years, as now seems quite reasonable, will cause little increase to the ice flux over the grounding line.

The ice shelves of the Antarctic Peninsula do, however, provide important and robust indicators of changing regional climate. They also provide the only available analogue for the larger Ronne/Filchner and Ross which we believe buttress and maintain WAIS. Understanding ice shelves and their potential breakup may provide the key to predicting the future of WAIS and its sea level change. The smaller, more accessible, and more rapidly changing ice shelves of the Antarctic Peninsula provide our best chance to study the processes, refine and tune the models and prepare ourselves to predict the future of WAIS.

6. Acknowledgements

My thanks extend to all my colleagues at the British Antarctic Survey who have helped in this work; most especially, Chris Doake, Rick Frolich and Liz Morris.

7. References

Bindschadler, R A (1990). SeaRISE: A multidisciplinary research initiative to predict rapid changes in global sea level caused by the collapse of marine ice sheets. NASA conference Publication 3075.

Doake, C S M (1975). Bottom sliding of a glacier measured from the surface. *Nature* **257** (5529), p. 780-782.

Doake, C S M (1982). The state of mass balance of the ice sheet in the Antarctic Peninsula. *Annals of Glaciology* **3**, p. 77-82.

Doake, C S M (1984). Glaciological evidence: Antarctic Peninsula, Weddel Sea. Glaciers, ice sheets, and sea level: effect of a CO₂-induced climatic change. US Department of Energy Report DOE/ER/60235-1, p. 197-209.

Doake, C S M and D G Vaughan (1991). Rapid

disintegration of Wordie Ice Shelf in response to atmospheric warming. *Nature* **350** (6316), p. 328-330.

Hughes, T J (1973). Is the West Antarctic Ice Sheet disintegrating? *Journal of Geophysical Research* **78**, p. 7884-7910.

Hughes, T J (1983). On the disintegration of ice shelves: the role of fracture. *Journal of Glaciology* **29**, p. 98-117.

Jezek, K C (1984). Recent changes in the dynamic condition of the Ross Ice Shelf, Antarctica. *Journal of Geophysical Research* **89**, p. 1925-1931.

Lange, M A and D R MacAyeal (1982). Numerical models of ice-shelf flow: ideal/real. *Annals of Glaciology* **12**, p. 97-103.

Lui, H W and K J Miller (1979). Fracture toughness of fresh-water ice. *Journal of Glaciology* **22**, p. 135-143.

MacAyeal, D R (1987). Ice-shelf backpressure: form drag versus dynamic drag. In *Dynamics of the West Antarctic Ice Sheet*. Eds C J Van der Veen and J Oerlemans. Pub. Reidel, Holland, p. 141-160.

MacAyeal, D R (1988). Can relict crevasse plumes on Antarctic Ice shelves reveal a history of ice-stream fluctuation? *Annals of Glaciology* **11**, p. 77-82.

MacAyeal, D R and R H Thomas (1982). Numerical modelling of ice shelf motion. *Annals of Glaciology* **3**, p. 189-194.

Mercer, J H (1978). West Antarctic Ice Sheet and CO₂ greenhouse effect: a threat of disaster. *Nature* **271** p. 321-325.

Morrison, S J (1990). Warmest year on record on the Antarctic Peninsula? *Weather* **45**, p. 231-232.

Muszynski, I and G E Birchfield (1987). A coupled marine ice-stream-ice-shelf model. *Journal of Glaciology* **33** (113) p. 3-16.

Oerlemans, J (1982). A model of the Antarctic Ice Sheet. *Nature* **297**, p. 550-553.

Pollard, D (1980). A simple parameterization of ice sheet ablation rate. *Tellus* **32**, p. 384-388.

Potter J R, J G Paren and J Loynes (1984). Glaciological and oceanographic calculations of the mass balance and oxygen isotope ratio of a melting ice shelf. *Journal of Glaciology* **30** (105), p. 161-170.

Reynolds, J M (1981). The distribution of mean annual

temperatures in the Antarctic Peninsula. *British Antarctic Survey Bulletin* **54**, p. 121-133.

Robin, G de Q (1974). Depth of water filled crevasses that are closely spaced. *Journal of Glaciology* **13**, p. 543.

Sabol, S A and E M Schulson (1989). The fracture toughness of ice in contact with fresh water. *Journal of Glaciology* **35**, p. 191-192.

Sansom, J (1989). Antarctic surface temperature time series. *Journal of Climate* **2**, p. 1164-1172.

Skvarca, P (in press). Fast recession of northern Larsen Ice Shelf monitored by satellite images. *Annals of Glaciology*.

Swithinbank, C W M (1988). Satellite image atlas of Glaciers of the World. USGS prof. pap., 1386-B.

Thomas, R H, T J O Sanderson and K E Rose (1979). Effect a climatic warming on the West Antarctic Ice Sheet. *Nature* **227**, p. 355-358.

Vaughan, D G, D R Mantripp, J Sievers and C S M Doake (in press). A synthesis of remote sensing data over Wilkins Ice Shelf, Antarctica. *Annals of Glaciology*.

Walford, M E R (1972). Glacier movement measured with a radio echo technique. *Nature* **239**, (5367), p. 93-95.

